Quantum complexity phase transitions in monitored random circuits

Ryotaro Suzuki[1], Jonas Haferkamp[1,2], Jens Eisert[1], and Philippe Faist[1]

[1]Dahlem Center for Complex Quantum Systems, Freie Universität Berlin, Berlin 14195, Germany
[2]School of Engineering and Applied Sciences, Harvard University, Cambridge, MA 02318, USA

arXiv:2305.15475v6 [quant-ph] 19 Jun 2025

Recently, the dynamics of quantum systems that involve both unitary evolution and quantum measurements have attracted attention due to the exotic phenomenon of measurement-induced phase transitions. The latter refers to a sudden change in a property of a state of n qubits, such as its entanglement entropy, depending on the rate at which individual qubits are measured. At the same time, quantum complexity emerged as a key quantity for the identification of complex behaviour in quantum many-body dynamics. In this work, we investigate the dynamics of the quantum state complexity in monitored random circuits, where n qubits evolve according to a random unitary circuit and are individually measured with a fixed probability at each time step. We find that the evolution of the exact quantum state complexity undergoes a phase transition when changing the measurement rate. Below a critical measurement rate, the complexity grows at least linearly in time until saturating to a value $e^{\Omega(n)}$. Above, the complexity does not exceed $\mathrm{poly}(n)$. In our proof, we make use of percolation theory to find paths along which an exponentially long quantum computation can be run below the critical rate, and to identify events where the state complexity is reset to zero above the critical rate. We lower bound the exact state complexity in the former regime using recently developed techniques from algebraic geometry. Our results combine quantum complexity growth, phase transitions, and computation with measurements to help understand the behavior of monitored random circuits and to make progress towards determining the computational power of measurements in many-body systems.

1 Introduction

The evolution of quantum complexity in many-body quantum systems offers a new approach to understand phenomena in quantum computation, quantum many-body systems, and black hole physics [1]: Complexity is able to capture the long-time behaviour of the quantum dynamics beyond the point where many physical quantities, such as the entanglement entropy, equilibrate to their limiting value [2, 3]. Quantum complexity might be viewed as a measure of the time for which a suitably chaotic system has been evolving [2]: Brown and Susskind conjectured that complexity grows linearly in time for generic quantum dynamics of an n-qubit system until saturating at times exponential in n [4]. In contrast, the entanglement entropy typically saturates after a time linear in n. Versions

Ryotaro Suzuki: ryotaro.suzuki@fu-berlin.de

of this conjecture have been proven in the context of random circuits [5–7]. Many recent results at the interface of quantum complexity and many-body systems have mainly been driven by the central role that quantum complexity appears to play in the *anti-de-Sitter space/conformal field theory* (AdS/CFT) correspondence [4, 8–11]: The quantum complexity of the quantum state in a CFT is believed to correspond to some physical property, such as the volume, of a wormhole contained in the corresponding AdS space [2, 12–14]. Overall, quantum complexity is a measure of the intricacy of the entanglement that is present in an n-qubit state; its physical and operational interpretations in the context of many-body physics are still being uncovered [4, 15–17].

To study the evolution of complexity of a CFT, one often resorts to the simpler model of local random quantum circuits, in which the evolution of an n-qubit system is modeled by applying 2-qubit gates chosen at random on neighboring qubits. Local random circuits are expected to reproduce a number of interesting features of chaotic systems [18–22] while being technically more convenient to analyze than chaotic Hamiltonian dynamics [23]. In the model of random quantum circuits, the quantum complexity has been proven to grow sublinearly in time until saturating at times exponential in n [5, 24, 25], using the toolbox of unitary t-designs [26, 27], where the quantum complexity is lower-bounded by $\Omega(\tau^a)$ with time τ and a positive number $a < 1$. The linear growth of the exact circuit complexity for local random quantum circuits was eventually proved in Ref. [6] by exploiting geometric arguments, where the exact complexity is lower-bounded by $\Omega(\tau)$ with time τ. More precisely, the toolbox of algebraic geometry enables a quantification of the dimension of the set of all possible unitaries that can be achieved with a fixed number of gates in a specific circuit layout. This dimension, called *accessible dimension*, yields a lower bound the exact quantum complexity of the random circuit. The main result of Ref. [6] is a consequence of the fact that the accessible dimension grows linearly in time until saturating at a time exponential in n (cf. also simplified proofs in Ref. [7]). We heavily rely upon this powerful mathematical toolkit in this work.

A different line of research at the interface of computational complexity theory and many-body physics concerns complexity phase transitions. The latter refer to situations where the complexity of solving a particular task undergoes a sudden and drastic change when a parameter in the problem is varied. Such complexity phase transitions have initially been discussed when studying the hardness regime of the random k-SAT problem [28, 29]. More recently, the complexity of classically simulating quantum circuits has been found to undergo a transition for *instantaneous quantum polynomial* (IQP) circuits [30–32], linear optical circuits [33–36], random quantum circuits [37, 38], and dual-unitary circuits [39–43]. Such transitions are of particular interest for drawing and delineating the boundaries between the power of classical and quantum computing [44].

Moreover, the effect of measurements on the dynamics of a complex many-body quantum system has drawn significant interest in the many-body physics community. A common model combining measurements and unitary evolution is a *monitored random quantum circuit* on n qubits and with measurement rate $p \in [0, 1]$: At each time step, randomly chosen two-qubit gates are applied between neighboring qubits; furthermore, each individual qubit undergoes a measurement in the computational basis with a probability p. This simple model has recently attracted substantial attention from the condensed matter physics community because such circuits may exhibit *measurement-induced phase transitions* [46, 47, 49–67]. The latter are an exotic type of phase transition that depends on the rate p at which measurements are performed: The state's entanglement entropy then commonly transitions from a scaling in the area of the region considered [45] at high p (the area law phase) to a scaling in the volume of the region at low p (the volume law

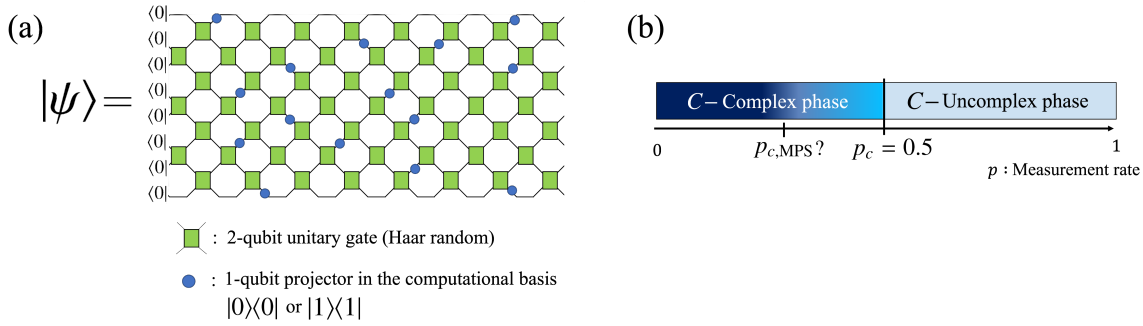

Figure 1: Our setup and the summary of the result. (a) We consider monitored random circuits consisting of two-qubit Haar-random gates (green boxes) arranged in staggered layers, where at each time step the individual qubits undergo a measurement in the computational basis (thick blue points) with probability p. The state vector $|\psi\rangle$ is obtained by applying the circuit onto the computational basis state vector $|0^n\rangle$ and conditioning on all the measurement outcomes. (b) We find that the complexity phase diagram of the monitored random circuit exhibits a phase transition at the critical measurement rate $p_c = 0.5$. The measure of complexity, $C(|\psi\rangle)$, is defined as the minimal number of two-qubit gates required to prepare $|\psi\rangle$ exactly, in any circuit layout. In the C-complex phase ($p < p_c$), the complexity C grows at least linearly until saturating to a value that is exponential in the system size. In the C-uncomplex phase ($p > p_c$), the quantity C saturates to a value $\mathrm{poly}(n)$ after a time no more than $O(\log(n))$. The result regarding the uncomplex phase agrees with earlier numerical results on the area law [45] of Rényi-0 entropy in the regime $p > p_c$ in Ref. [46]. Moreover, another earlier numerical result [47] points to a description of the state vector $|\psi\rangle$ in terms of a *matrix-product state* (MPS) [48] with $\mathrm{poly}(n)$ bond dimension in the region $p \geq p_{c,\mathrm{MPS}}$, with $p_{c,\mathrm{MPS}} < 0.5$. Given that a robust measure of complexity would saturate after a time $\sim \mathrm{poly}(n)$ in this region, it is likely the region $p_{c,\mathrm{MPS}} < p < p_c$ yields examples of states generated by monitored random circuits whose exact complexity grows to large values yet remain close in trace norm to a state of low complexity.

phase).

The goal of our work is to combine the ideas of (i) complexity growth in many-body systems, (ii) complexity phase transitions, and (iii) measurement-induced phase transitions, to prove the existence of a sharp transition in the evolution of quantum complexity in monitored quantum circuits depending on rate at which measurements are applied. We thereby introduce the distinct notion of quantum state complexity into the study of monitored quantum circuits.

Specifically, we prove rigorously that the growth of the exact state complexity in a monitored random circuit on n qubits makes a sharp transition at a critical rate $p_c = 0.5$ at which measurements are applied (sketched in Fig. 1). Below the threshold, the quantum complexity grows at least linearly in time until saturating to a value $e^{\Omega(n)}$ (the *complex phase*). Above the threshold, the state's complexity saturates to a value $\mathrm{poly}(n)$ after a time no more than $O(\log(n))$ (the *uncomplex phase*). We quantify the state's quantum complexity in terms of the number of two-qubit unitary gates required to prepare that state exactly.

We establish a framework of the study of complexity of monitored random circuits as follows. We draw deep inspiration from the seminal work on measurement-induced phase transitions in the dynamics of entanglement [46], including the use of techniques from percolation theory [68], while adapting to the techniques to lower bound the exact quantum circuit complexity using semi-algebraic geometry of Ref. [6]. The complexity phase transition that we find concerns the quantum complexity of the output state of the monitored circuit, and might be of different nature than the phase transition in the classical complexity of sampling outcomes from random circuits [38] and monitored linear

optical circuits [36]. Our results reinforce monitored random circuits as a promising model to investigate quantum complexity phase transitions and the influence of measurements on the complexity of a quantum circuit's output state.

The remainder of this work is organized as follows. In Section 2, we review monitored quantum circuits and methods of lower-bounding the state complexity. In Section 3, we summarize our main results, discuss their core implications, and sketch our proof strategy. In Section 4, we give a proof of our main result. Section 5 is devoted to conclusion and discussion.

2 Setting

In this section, we review the definitions of monitored random quantum circuits, of the exact state complexity, and of the accessible dimension.

2.1 Monitored random quantum circuits

Throughout this work, we consider a system of n qubits. The qubits might be realized, for instance, as individual spins of a quantum many-body system. For technical convenience, we assume that n is an even number. The computational basis of the system is denoted by $|i_1, i_2, \ldots, i_n\rangle$, where $i_j = 0, 1$ indicates the state of the j-th qubit. A *monitored random quantum circuit with measurement rate* $p \in [0, 1]$ is a quantum circuit with staggered layers of two-qubit gates on nearest neighbors, or the brick-wall architecture, in which each qubit has a probability p at each time step to be measured in its computational basis and be projected into the resulting outcome [Fig. 1(a)]. It is defined as

$$V^M(t) := \prod_{\tau=1}^{t/2} M(2\tau)U^{(e)}(2\tau)M(2\tau-1)U^{(o)}(2\tau-1), \tag{1}$$

where

$$U^{(o)}(2\tau-1) := \prod_{i=1}^{\frac{n}{2}} U_{2i-1,2i}(2\tau-1), \tag{2}$$

$$U^{(e)}(2\tau) := \prod_{i=1}^{\frac{n}{2}-1} U_{2i,2i+1}(2\tau), \tag{3}$$

$$M(\tau) := \prod_{i=1}^{n} M_i(\tau). \tag{4}$$

Here, t is an even number, $U_{i,j}(\tau)$ is a Haar-random unitary gate acting on qubits i and j at time τ, and $M_i(\tau) \in \{\sqrt{1-p}I_i, \sqrt{p}\,|0\rangle\langle 0|_i\,, \sqrt{p}\,|1\rangle\langle 1|_i\}$. The latter are Kraus operators of the channel that implements a measurement in the computational basis with probability p. We say that the qubit i is *measured* at time τ if $M_i(\tau)$ is either $\sqrt{p}\,|0\rangle\langle 0|_i$ or $\sqrt{p}\,|1\rangle\langle 1|_i$. The *measurement configuration* $M := \{M_i(\tau)\}_{i,\tau}$, is the collection of all measurement outcomes at each space-time point of the circuit. By construction, M contains all the information about the layout of the circuit, including n and t, along with which qubits were measured at which time, and what the projective measurement outcomes were. Note that the time evolution operator $V^M(t)$ in Eq. (1) is *not* unitary, i.e.,

$$V^M(t)^\dagger \neq V^M(t)^{-1}, \tag{5}$$

except in the situation when the measurement rate p is exactly zero. That $V^M(t)$ is not unitary corresponds to the fact that we measure the system and condition the evolution on the measurement outcomes specified by M.

Our results concern the output of a monitored quantum circuit when it is applied onto the initial state vector $|0^n\rangle$. The state vector $V^M(t)\,|0^n\rangle$ represents the unnormalized output of the monitored quantum circuit, projected according to the measurement configuration M. Its squared norm $\langle 0^n|V^M(t)^\dagger V^M(t)|0^n\rangle$ is the probability that a measurement configuration M is observed for fixed choices of gates $U_{i,j}(\tau)$. Our results concern the complexity of the normalized output quantum state vector

$$\left|\phi^M\right\rangle := \frac{V^M(t)\,|0^n\rangle}{\|V^M(t)\,|0^n\rangle\|}\ . \tag{6}$$

This state is the output of the monitored quantum circuit after conditioning on the measurement outcomes M.

2.2 State complexity

The complexity of a quantum state vector $|\psi\rangle$ refers to the minimal number of elementary operations, such as two-qubit gates, that need to be composed in order to prepare $|\psi\rangle$ starting from the reference state vector $|0^n\rangle$. The complexity of a state is ordinarily defined by considering two-qubit unitary gates as the elementary operations. We call this complexity measure the *C-complexity*:

Definition 1 (Exact C state complexity)**.** *The* C state complexity *of a normalized state vector $|\psi\rangle$ is the minimal number of two-qubit gates required to prepare $|\psi\rangle$ from the state vector $|0^n\rangle$. The gates can be any elements of $SU(4)$ and the circuit may have any chosen connectivity.*

We also consider a stronger notion of complexity in which the elementary operations also include measurements with post-selection [69]. A post-selected circuit is defined as a quantum circuit consisting of two-qubit unitary gates and single-qubit measurements in the computational basis where the measurement outcomes are post-selected to the desired measurement outcomes, for example, 0 for all outcomes. At any time in a post-selected circuit, arbitrary qubits, for instance the i-th qubit, of a state vector $|\psi\rangle$ can be measured in the computational basis and be post-selected to the desired measurement outcome 0, resulting in the state $(\|\langle 0|_i\,|\psi\rangle\|)^{-1}|0\rangle\langle 0|_i\,|\psi\rangle$. The exact state complexity C with post-selected circuits is defined as follows:

Definition 2 (Exact C_m state complexity)**.** *For a state vector $|\psi\rangle$ with $0 < \langle\psi|\psi\rangle \leq 1$, the exact C_m state complexity $C_m(|\psi\rangle)$ is the minimal number of two-qubit gates in an arbitrary post-selected circuit that prepares $(\||\psi\rangle\|)^{-1}\,|\psi\rangle$ from the initial state vector $|0^n\rangle$. The post-selected circuit consists of two-qubit unitary gates with arbitrary connectivity and where an arbitrary number of single-qubit computational basis measurements can be applied, with post-selection on a desired outcome, at any space-time points of the circuit.*

The set of post-selected quantum circuits includes unitary circuits as a special case, implying that the measure of complexity C_m is a lower bound on the usual state complexity C.

2.3 Accessible dimension

The *accessible dimension* [6] has been defined as the dimension of the set of all possible unitary circuits that can be achieved with a fixed circuit layout, by varying the individual choices of the gates in that circuit. Here, we adapt this definition to our setting, and show that it serves lower-bounds, analogously to the proof in Ref. [6], on the C- and C_m-complexity of a monitored random circuit below the critical measurement probability. For a monitored random circuit with a fixed measurement configuration M, we define the *contraction map* from a collection of two-qubit unitary gates to the output state as

$$F^M : [\mathrm{SU}(4)]^{\times R} \to B_1^{2\times 2^n} \subset \mathbb{C}^{2^n}, \tag{7}$$

$$F^M(U_1, U_2, \ldots, U_R) = V^M(t)\,|0^n\rangle\,, \tag{8}$$

where $B_1^{2\times 2^n}$ is the real unit ball with the center at the origin, where R is the total number of two-qubit unitary gates in the monitored random circuit specified through M, and where each two-qubit unitary gate in Eq. (1) is set to the corresponding unitary U_j. That the image of F^M includes sub-normalized n-qubit states is a consequence of $V^M(t)$ not being unitary. We denote the image of F^M by $\mathcal{S}^M$, that is, the set of all output states generated by the monitored random quantum circuit with M. (See additional technical details in Appendix A.)

We define the *rank* of F^M as the number of independent degrees of freedom required to specify a perturbation of the image of F^M when we perturb the gates $\{U_1, \ldots U_R\}$. More specifically, the rank of F^M at a point $\{U_1, U_2, \ldots, U_R\}$, denoted by $\mathrm{rank}_{U_1,\ldots,U_R}(F^M)$, is defined by the dimension of the real linear space spanned by the set of output state vectors

$$\{F^M(U_1, \ldots, (\alpha \otimes \beta)U_j, \ldots, U_R)\}_{j,\alpha,\beta}, \tag{9}$$

where $j \in \{1, 2, \ldots, R\}$ and $\alpha,\ \beta \in \{I, X, Y, Z\}$ are Pauli operators such that $(\alpha, \beta) \neq (I, I)$. We then define the *accessible dimension* as the maximal rank of F^M over all unitary gates:

Definition 3 (Accessible dimension)**.** *For a monitored random quantum circuit with a measurement configuration M, the accessible dimension d_M is the maximal rank of F^M over all two-qubit unitary gates $\{U_1, U_2, \ldots, U_R\}$, where $U_j \in SU(4)$.*

A strategy to lower bound the accessible dimension d_M is to lower bound the rank of F^M at any chosen point $\{U_1, \ldots U_R\}$. The accessible dimension d_M is also the dimension of the set $\mathcal{S}^M$ (see Appendix A). We prove that the complexity measure C_m is lower bounded in terms of d_M, which is analogous to the proof in Ref. [6].

Lemma 4 (Complexity by dimension)**.** *Let $|\psi\rangle \in \mathcal{S}^M$ be distributed according to the output of a monitored random quantum circuit with a fixed measurement configuration M, in which all unitary gates are chosen at random from the Haar measure. Then $C_m(|\psi\rangle) \geq (d_M - 3n - 2)/11$ with unit probability.*

In the above lemma, given a measurement configuration of a monitored circuit M, the accessible dimension has been shown to take the maximum value over all unitary gates except for a measure zero set. The above lemma serves in our proof to reduce the problem of finding a lower bound on C_m for a monitored random quantum circuit to finding a lower bound on d_M.

3 Main result: Complexity phase transition in monitored random quantum circuits

We prove that both of the C- and C_m-complexity of the output state of a monitored random quantum circuit exhibit a phase transition at a critical measurement probability $p_c = 0.5$.

Theorem 5 (Complexity growth in monitored circuits)**.** *Let $|\psi\rangle$ be the output state vector of the monitored random circuit with measurement rate p, conditioned on the outcomes of the measurement that were applied in the monitored circuit. If $p < p_c$, $C(|\psi\rangle)$ and $C_m(|\psi\rangle)$ grow at least linearly and linearly in t, respectively, until they saturate to values $e^{\Omega(n)}$, with probability $1 - e^{-\Omega(n)}$. If $p > p_c$, and for any $0 < \epsilon < 1$, we have $C(|\psi\rangle) \leq \mathrm{poly}(n/\epsilon)$ and $C_m(|\psi\rangle) \leq O(n \log(n/\epsilon))$ except with probability at most ϵ.*

Our bounds on both complexities do not depend on the specific measurement outcomes M, even though the output state vector $|\psi\rangle$ is conditioned on M.

Our proof exploits techniques from percolation theory [68] to prove a sharp transition between these two regimes at the critical measurement rate $p_c = 0.5$. Above this rate, measurements percolate across the width of the circuit, periodically resetting the state's complexity. This implies the upper bound of the complexity by $\mathrm{poly}(n)$. Below the critical rate, it turns out multiple paths without any measurements can percolate along the length of the circuit, supporting a computation whose complexity grows linearly in time until times exponential in n. The growth of $C(|\psi\rangle)$ in the regime $p < p_c$ follows from the general bound $C_m(|\psi\rangle) \leq C(|\psi\rangle)$.

Our core technical result is a lower bound on the accessible dimension of a monitored random quantum circuit in the regime $p < p_c$ By Lemma 4, this bound immediately translates into a corresponding bound on the C_m-complexity.

Lemma 6 (Growth of the accessible dimension in monitored circuits)**.** *If $p < p_c$, d_M grows linearly in t until an exponential time $t = e^{\Omega(n)}$ with probability $1 - e^{-\Omega(n)}$.*

We now provide a sketch of the proof of Lemma 6. Two separate arguments are developed in the regimes $p > p_c$ and $p < p_c$. In the regime $p > p_c = 1/2$, percolation theory states that measurements will regularly percolate throughout the width of the circuit, resetting the state vector to $|0^n\rangle$ along those paths (Fig. 3(a)). Such measurement percolation occurs within the last n layers of gates in the monitored circuit with probability $1 - e^{-\Omega(n)}$, meaning that the set of output states of the circuit cannot have the C_m-complexity cannot exceed $O(n^2)$. The argument can be further reinforced to upper-bound C-complexity by $\mathrm{poly}(n)$, and to bound the C and C_m complexity measures in the case where the tolerated failure probability is arbitrary.

In the regime $p < p_c = 1/2$, we lower-bound the accessible dimension as follows. We first show that for a fixed configuration of measurements M, there are paths without any measurements that percolate throughout the length of the circuit. We call such paths *measurement-free paths*. Then we show that these paths can be used to run an exponentially long quantum computation. The main challenge is to construct an embedding of an arbitrary quantum circuit on $\Omega(n)$ qubits and of depth $\Omega(t)$ into the monitored random quantum circuit with a fixed configuration of measurements M. The main idea of the embedding is to associate one qubit of the $\Omega(n)$ sized circuit to a measurement-free path, and to choose the gates of the monitored random circuit so that they ensure the qubit's information is carried along the measurement-free path and that they implement the gates of the $\Omega(n)$ sized circuit on those qubits. There are two specific challenges that one faces

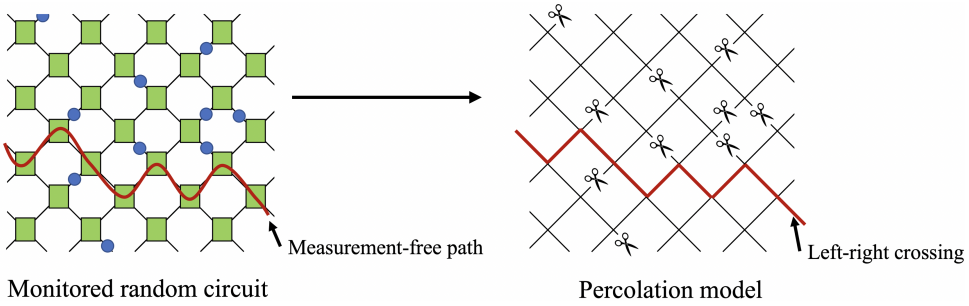

Figure 2: A mapping from the bond structure of a monitored random circuit to a percolation model. Each measured and unmeasured bond is mapped to closed (with scissors) and open edge (without scissors), respectively.

when constructing this embedding: One must show that (a) the computation can proceed even if a measurement-free path is not *causal*, i.e., if it momentarily wraps back in time by following legs between gates in a direction opposite to the circuit's time direction, and (b) two-qubit gates can be implemented between two such paths (Fig. 3(b)). Challenge (a) is addressed as follows. If a measurement-free path follows a leg of a unitary gate in a direction contrary to the circuit's forward time direction, then we can exploit the existence of a measurement immediately after that gate to teleport the qubit being carried by the path further along the path, even if the information is carried backwards with respect to the circuit's direction. This is possible because the measurement configuration M is fixed, meaning that the measurement immediately after the gate has a predetermined outcome onto which the state is projected. To address challenge (b), we exploit the fact that paths with no measurements also percolate vertically across the width of the circuit; these paths can be used to implement a CNOT gate across two measurement-free paths using a teleportation-based scheme.

Both arguments addressing challenges (a) and (b) rely on the existence of measurements on certain qubits that are neighboring the measurement-free path. Yet such measurements might not always exist at the desired locations. We prove that for any measurement configuration M, one can always select additional qubits to be measured without increasing the accessible dimension of the monitored random circuit. Therefore, should a measurement at a given location be required by our embedding scheme, it can always be added if necessary while still yielding a lower bound on the accessible dimension of the monitored circuit in the original measurement configuration. We believe that the following lemma might be of independent interest, as it provides a rigorous quantitative statement about the impossibility of measurements to increase a quantity, the accessible dimension, which is a proxy quantity for complexity for monitored random circuits.

Lemma 7 (Measurements cannot increase the accessible dimension)**.** *Let M be a measurement configuration, and let M' be a configuration obtained by changing some space-time locations in M from being unmeasured to being measured. Then $d_{M'} \leq d_M$.*

Intuitively, the dimension of the set of states generated by a random monitored circuit for a given measurement configuration cannot increase if one inserts an additional projector in the circuit. We present a proof of this statement as Lemma 16 in Appendix B.

4 Proof of the main result

In this section, we prove Theorem 5. A central ingredient of our proof is the use of techniques from percolation theory. We briefly review these techniques in Section 4.1. We then apply these techniques in Section 4.2 to obtain an upper bound on the C complexity in the regime $p > p_c$. Finally, we complete the proof of Theorem 5 in Section 4.3 by proving a lower bound on the C complexity in the regime $p < p_c$.

4.1 Percolation theory

In percolation theory, we consider a graph whose edges can be in one of two states, open or closed, where the state of each edge is chosen to be open or closed independently with probability q and $1-q$, respectively [68]. Bond percolation theory is concerned with the existence or absence of a path consisting of connected open edges in the graph. A well-studied setting is the existence of a path that crosses from left to right in a $L \times L$ square lattice while passing only through open edges. In the large L limit, there is a critical probability q_c below which there does not exist a left-right crossing with the probability $1 - e^{-\Omega(L)}$, but above which such crossings appear with probability $1 - e^{-\Omega(L)}$. Moreover, for a square lattice in two spatial dimensions, the critical probability is $q_c = 1/2$. We refer to Appendix D for a more in-depth review of percolation theory, including percolation on rectangular lattices.

Our application of percolation theory follows similar techniques used to compute the Rényi-0 entropy in Ref. [46]. In order to formally apply techniques from percolation theory to monitored random quantum circuits, we map a monitored random circuit to a graph with edges that are randomly open or closed. We define a graph by mapping each two-qubit unitary gate and its unmeasured bonds to a vertex and the open edges incident with it, respectively (Fig. 2). With this mapping, the measurement rate p is equal to the probability of closing an edge $1-q$. Moreover, percolation results for the square lattice extend naturally to the diagonally tilted square lattice as in Fig. 2, given that percolations from the left to the right of the tilted lattice can be constructed from left-right and top-bottom percolations on the original, untilted lattice (cf. Appendix D).

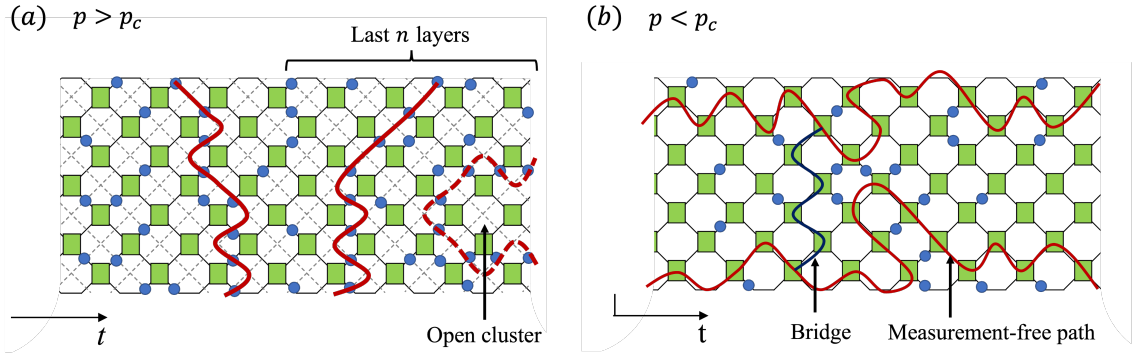

Figure 3: Monitored random circuits above and below the critical measurement probability. (a) Above the threshold, paths of measurements cut across the circuit from top to bottom. Their effect is to reset the state along the path to a product state, whose complexity vanishes. The region delimited by the red broken line is an example of an *open cluster*. (b) Below the threshold, a linear number of measurement-free paths cross from the beginning to the end of the circuit. These paths can be used to embed a unitary circuit into the monitored circuit. A bridge (black line) is a vertical path of open edges used to implement two-qubit gates in the embedded unitary circuit.

4.2 The uncomplex phase

As a warm-up and to build additional intuition with the proof techniques we use, we first provide a simple upper bound on the C_m-complexity in the regime $p > p_c$: Consider a circuit of depth $t > n$, and consider the last n layers of that circuit. Our strategy is to use percolation theory to conclude that there exist measurements that cut through the width of the circuit in those last n layers, resetting the state vector to $|0^n\rangle$ at the location of those measurements [Fig. 3 (a)]. We apply percolation theory to the dual lattice of the percolation model introduced in Fig. 2, depicted in Fig. 3 (a). For $p > p_c$, percolation theory states that with probability $1 - e^{-\Omega(n)}$ there exist paths of measurements in the dual lattice that connect the top of the circuit with the bottom side of the circuit. For such a path, there is no unmeasured bond connecting the gates on the left side of the path to the gates on the right side of the path. (This property would not have been guaranteed had we applied percolation theory directly to the graph in Fig. 2 rather than to its dual lattice.) The measurements therefore reset the state vector along the path to $|0^n\rangle$. Since there are at most $O(n^2)$ gates after this path, both the accessible dimension d_M as well as the output state complexity $C_m(|\psi\rangle)$ cannot exceed $O(n^2)$. Therefore, if $p > p_c$, then $C_m \leq O(n^2)$ except with probability $e^{-\Omega(n)}$.

We now present our the part of the proof of Theorem 5 pertaining to the uncomplex phase. Our proof proceeds by upper bounding the size of regions consisting of connected open edges, or *open clusters*, on the graph in Fig. 2. Open clusters correspond to connected bonds of gates in the circuit which are not measured (inside the broken line in Fig. 3 a). The output state only depends on the unitary gates whose bonds are in the open clusters and contain the boundary at the final time. Indeed, single-qubit measurements at the boundary of the open clusters reset each qubit to $|0\rangle$. There are no more than $n/2$ open clusters containing the bonds at the final time. We now upper bound the size of such open clusters by $O(\log(n))$. Let $\{C_i\}_1^m$, where $m \leq n/2$, be the set of the distinct open clusters containing the bonds at the final time and $|C_i|$ be the number of edges, or bonds, in $C_i, i \in \{1, 2, \ldots, m\}$. Then, the following lemma holds.

Lemma 8 (Small unmeasured regions)**.** *Assume $p > p_c$. For any $0 < \epsilon < 1$, it holds:*

$$|C_i| = O\left(\log\left(\frac{n}{\epsilon}\right)\right), \tag{10}$$

for all $i \in \{1, 2, \ldots, m\}$, with probability $1 - \epsilon$.

We give a proof of the above lemma in Appendix D.2 (stated there as Lemma 19). Because of Lemma 8, the output state is generated by a $O(\log(n/\epsilon))$-depth post-selected quantum circuit, implying that $C_m \leq O(n \log(n/\epsilon))$ with probability $1 - \epsilon$. Moreover, it indicates that the Schmidt rank of the output state in any bi-partition is $\mathrm{poly}(n/\epsilon)$, implying that the output state can be efficiently represented by a *matrix product state* (MPS) [48], and therefore it is prepared by a unitary circuits with $\mathrm{poly}(n)$ complexity [70, 71]. Overall, for the output state vector $|\psi\rangle$, our argument gives upper bounds $C(|\psi\rangle) \leq \mathrm{poly}(n/\epsilon)$.

This proof also recovers the upper bound for C_m obtained in our initial percolation argument (cf. warm-up proof above) when ϵ is chosen exponentially small. Plugging $\epsilon = e^{-cn}$ for fixed $c > 0$ yields the upper bound $C_m \leq O(n \log(n) + cn^2) = O(n^2)$.

4.3 The complex phase

The C-complex phase refers to the phase in which the C complexity grows at least linearly

until saturating to a value $e^{\Omega(n)}$. We show that this phase occurs in monitored random circuits whenever $p < p_c$.

Our proof proceeds as follows. For a fixed measurement configuration M, the goal is to prove a lower bound on the accessible dimension d_M in order to apply Lemma 4. The strategy to lower bound d_M is to show that, for some $m = \Omega(t)$, it is possible to embed any depth-m unitary circuit with arbitrary single-qubit gates and CNOT gates into a set of paths along the monitored quantum circuit that avoid measurements. We then show that the accessible dimension of such unitary circuits grows linearly in m, thereby showing that $d_M = \Omega(m)$. The bulk of this section is concerned with constructing such an embedding.

When $p < p_c$, there are $\Omega(n)$ measurement-free paths even for exponentially long monitored random quantum circuits:

Lemma 9 (Existence of measurement-free paths)**.** *If $p < p_c$, there exist $\Omega(n)$ disjoint measurement-free paths that percolate throughout the length of the circuit in time $e^{\Omega(n)}$, with probability $1 - e^{-\Omega(n)}$.*

We give a proof of Lemma 9 in Appendix D.1.2 (stated as Lemma 18). Without loss of generality, we can assume that all measurement outcomes in the monitored circuit are 0 without changing the accessible dimension associated with the measurement configuration M. Indeed, the gates are chosen at random from the unitarily invariant Haar measure on $SU(4)$; thus, for any measurement outcome 1, we can map the setting to an equivalent one where the measurement is 0 and where additional X gates are applied immediately before and immediately after that measurement.

We now seek to construct an embedding of a quantum unitary circuit of $\Omega(n)$ qubits into the monitored random quantum circuit, where each measurement-free path carries one qubit of the unitary circuit. We first construct this embedding in a simpler situation with some additional convenient assumptions. We then present the embedding in the general case, lifting all the simplifying assumptions.

Let us assume that all measurement-free paths always traverse gates from an input leg of the gate to an output leg of the gate. Following such measurement-free paths, one does not go back in the time direction, and we say the paths are *causal*. Each path is assigned to carry one qubit while avoiding measurements. We apply the identity gate or the SWAP gate so that the qubit state follows the legs of the path (Eq. (11)). In this way, qubit states are transferred along the measurement-free paths without being measured. We can apply an arbitrary single-qubit gate to the qubit by multiplying a single-qubit gate to the identity gate or the SWAP gate. Let us furthermore assume that nearest neighbour paths meet at some points, that is, nearest neighbour paths include the legs of the same unitary gates, and the number of the unitary gates is $\Omega(t)$ for each path. At the point two paths meet, we can apply a CNOT gate, which results in performing a CNOT gate on the two qubits carried by the nearest neighbour paths. The two-qubit gates which are outside the measurement-free paths are chosen to be identity gates. The case described above is graphically exemplified as

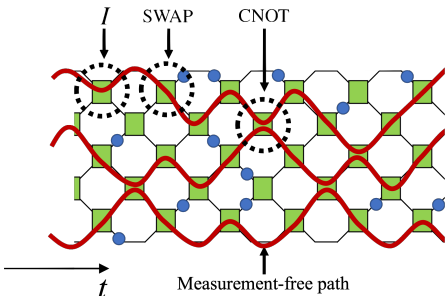

. (11)

Here, there are three such paths, i.e., it simulates a unitary circuit with three qubits, and we apply the suitable two-qubit gate along the paths and at the points they meet, for example we applied I, SWAP, CNOT in the broken circles as shown. Single-qubit gates can be multiplied into these two-qubit gates to enable universal computation in the embedded unitary circuit.

In the above setting, the output states at the end of measurement-free paths is equal to a state generated by a depth-$\Omega(t)$ unitary circuit consisting of single-qubit gates and CNOT gates with the brick-wall architecture. Because arbitrary single-qubit gates and CNOT gates form a universal gate set [72], we can embed a universal unitary circuit into a monitored circuit with such a measurement configuration M. Let S^0 be the set of the output states of a random unitary circuit with the brick-wall architecture and two-qubit random unitary gates

$$U = (u_1 \otimes v_1)\, W\, (u_2 \otimes v_2)\,, \tag{12}$$

where $u_{1,2}$, $v_{1,2}$ are Haar random single-qubit gates and W is chosen from $\{I,\ \mathrm{CNOT}\}$ uniformly randomly. We denote by d_0 the accessible dimension of S^0, where the accessible dimension of the random unitary circuit is defined as per Definition 3 with a measurement configuration that contains no measurements and with single-qubit perturbations: $(\alpha, \beta) = (I, \sigma), (\sigma, I)$ for $\sigma \in \{X, Y, Z\}$ in Eq. (9). The reason for the restriction of the perturbations to single-qubit gates is because only single-qubit gates in Eq. (12) are parametrized continuously and can be, therefore, perturbed. Then, because the perturbed output states of the random unitary circuit are equal to some perturbed output states of the monitored random circuit in Eq. (9) with M simulating the random unitary circuit, up to real scalar factors, we obtain the inequality

$$d_M \geq d_0. \tag{13}$$

Then, we use an argument following Ref. [6] to lower bound d_0. We specify the depth of the unitary circuit by $d_0(t)$, which is d_0 of depth-t random unitary circuits defined above. Then we prove the following lemma.

Lemma 10 (Lower bound on d_0)**.** *Let $t \geq 0$ be an integer. Then, d_0 grows linearly in depth as*

$$d_0(t) \geq \left\lfloor \frac{2t}{3n} \right\rfloor, \tag{14}$$

until it saturates in a depth exponential in n.

We give a proof of Lemma 10 in Appendix A (stated as Lemma 15). Moreover, with Lemma 4, it implies that $C_m(|\psi\rangle)$ and $C(|\psi\rangle)$, where $|\psi\rangle$ is an output state vector of monitored random circuits with the above measurement configurations, also grows linearly and at least linearly in t, respectively, until saturating to a value $e^{\Omega(n)}$.

What is left to be shown is that a unitary circuit can be embedded to a monitored circuit with the general conditions, such that measurement-free paths are not always causal, and they do not meet at some space-time points. First, we generalize the embedding to the case where measurement-free paths are not causal, that is, the paths include the legs of two inputs or two outputs of a two-qubit unitary gate. For now, we assume that there are measurements at the points where the path changes the time direction (the broken circles in Eq. (15)). (We discuss below how to remove this assumption using Lemma 7.)

In this case, the path is graphically shown as

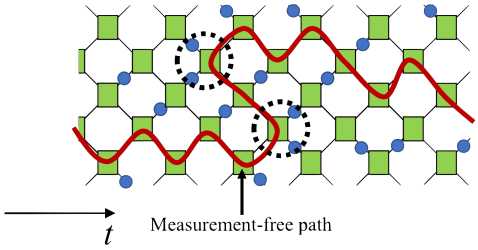

, (15)

where we marked with broken circles at which the path changes the time direction. Still, the qubit state can be protected from the measurements by using a scheme similar to the entanglement teleportation. To see this, we need the following simple equality: If we choose the two-qubit gate as $U = \mathrm{CNOT}(H \otimes I)$, then we have

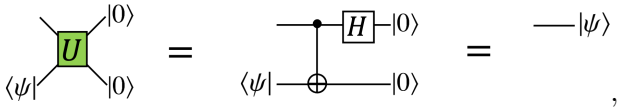

, (16)

where we have omitted the constant factor in the last equality, which is not important for our proof. Here, we can interpret it as the measurement in the Bell basis, with a post-selection on the outcome. With Eq. (16) in mind, we fix the unitary gate at which the path changes direction to go backwards in time (the bottom broken circle in Eq. (15)) so that the qubit state is measured in the Bell basis. We also fix the unitary gate at which the path changes direction to go forwards again in time (the top broken circle in Eq. (15)) so that a Bell state is prepared. The qubit state can therefore be transferred along the path, i.e., the input state of the measurement-free path is equal to its output.

Next, we discuss how to apply a CNOT gate between two nearest-neighbour paths which do not share a unitary gate, and give a lower-bound on the number of CNOT gates that can be performed. Here, we make use of measurement-free paths which percolate through the width of the circuit, i.e., from the top to the bottom. To perform a CNOT gate, we are only interested in a segment of the top-bottom measurement-free paths between the two paths carrying the quantum state, and we call such segment *bridge*. They are graphically exemplified as

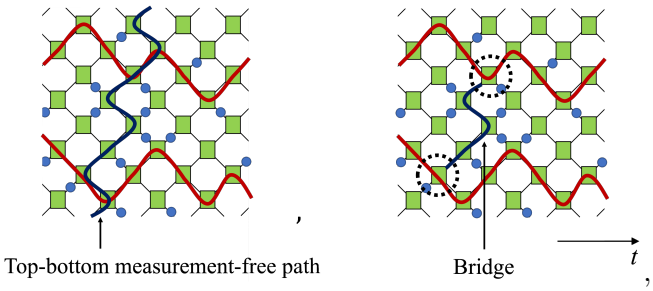

, (17)

where the red lines are the paths carrying two-qubit state. For now, we assume again that there are measurement at the following desired locations: (1) the legs of the unitary gates at which the top-bottom paths change direction in time (analogous to the broken circles in Eq. (15)) and (2) the fourth leg of the unitary gates at the intersection of the horizontal measurement-free paths and the top-bottom measurement-free path (the broken circles in Eq. (17)). If we fine tune the unitary gates along the bridge, we can perform a

CNOT gate between nearest-neighbour measurement-free paths. Specifically, we choose the unitary gates along a bridge such that the bridge protects a qubit state from being measured as with the unitary gates in the measurement-free paths, using a SWAP gate or an identity gate if the bridge traverses the gate from an input leg to an output leg, or the scheme in Eq. (16) if the bridge traverses the gate through two input legs or through two output legs. Also, for two unitary gates at the edge of the bridge (the broken circles in Eq. (17)), we choose them as CNOT and CNOT$(I \otimes H)$ or $(I \otimes H)$CNOT, possibly multiplied by SWAP if required to ensure the qubit continues to be transferred along the horizontal measurement-free path. The target qubit of CNOT and the order of $I \otimes H$ and CNOT depend on the locations of legs belonging to the bridge and the path at the edge of the bridge, i.e., the shape of the path and the bridge in the broken circles in Eq. (17). In the example in Eq. (17), CNOT is performed as

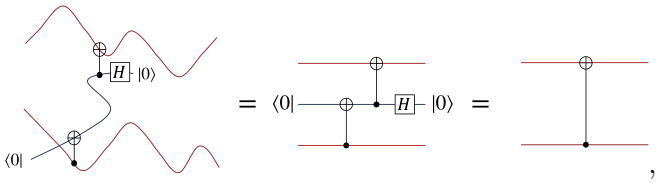

, (18)

where we chose the unitary gates along measurement-free paths and inside the bridge as the specific ones so that they carry qubit states, we apply $(I \otimes H)$CNOT and CNOT at the edge of the bridge, and we omit the constant factor in the last equality. Other bridge configurations, such as if the bridge is attached on both ends to input legs of unitary gates on the horizontal measurement-free paths, can be treated similarly (cf. Appendix C).

For every of the n time steps, that is every of the squares of the monitored circuit from $(i+1)$-th time step to $(i+n)$-th time step, where i is a multiple of n, there are $O(n)$ top-bottom measurement-free paths with probability $1 - e^{-\Omega(n)}$ (Fact 3 in Appendix D) until an exponential number of time steps in n. Then, we can apply $\Omega(t)$ layers of CNOT gates with the brick-wall architecture using the bridges made by the top-bottom paths. We can therefore embed any depth-m unitary circuit, where $m = \Omega(t)$, with arbitrary single-qubit gates and CNOT gates into a monitored circuit with such measurement configuration.

In the discussion above, we have assumed that there are measurements at certain desired locations: around the points where the measurement-free paths and the bridges change direction in time, and on the fourth leg of each junction of the paths and the bridges. Below, we show how a lower-bound on the accessible dimension is obtained without the measurements at the desired locations. We consider a measurement configuration M which does not include measurements at such locations. Then, we set up another configuration M' by adding measurements to M at the desired locations. Here, by adding measurements, we mean that M' is made by changing some $\sqrt{1-p}I$ in M to projections $\sqrt{p}\,|0\rangle\langle 0|$ or $\sqrt{p}\,|1\rangle\langle 1|$. Because we have assumed that the measurement outcomes are all 0, we replace $\sqrt{1-p}I$ by $\sqrt{p}\,|0\rangle\langle 0|$. For example, we add measurements to the points which a measurement-free path changes the time direction as

. (19)

Then, using Eq. (16) again, a qubit state can be transferred along the path with the measurement configuration M' in Eq. (19). A key lemma to lower-bound d_M by considering

M' is that the accessible dimension cannot increase by adding measurement (Lemma 7): If M' is made up by adding measurements to M, then $d_{M'} \leq d_M$. Therefore, a lower-bound on $d_{M'}$ immediately implies one on d_M. However, adding measurements to qubits neighboring a measurement-free path might inadvertently break another measurement-free path in the circuit. Such a situation can occur if a measurement-free path shares a unitary gate with a nearest-neighbour path at which it changes direction in time. Still, the number of measurement-free paths that survive after adding the required measurements remains $\Omega(n)$ because we can pick up at least half of the paths in M such that any pair of two paths do not share the same unitary gates.

In summary, a depth-t monitored circuit with M', where measurement are added at the desired locations, can simulate a depth-$\Omega(t)$ unitary circuit, which implies that $d_{M'} = \Omega(t)$. This lower-bound holds until an exponential time in n, because linear number of measurement-free paths in n and linear number of bridges in t exist until then with probability $1 - e^{-\Omega(n)}$ Then, because $d_{M'}$ lower-bounds d_M, we obtain $d_M = \Omega(t)$, which means that the accessible dimension of a monitored circuit with measurement rate $p < p_c$ grows linearly in t until a time $e^{\Omega(n)}$.

5 Conclusion and discussion

Our work combines techniques from quantum complexity and monitored quantum circuits to show that the quantum complexity of a state — akin to other physical quantities including the entanglement entropy — undergoes phase transitions in a many-body system subject to measurements. Our results, therefore, contribute to reinforcing the interpretation of quantum complexity as a meaningful physical quantity, given its ability to identify different regimes of behavior of the evolution of a quantum many-body system. Indeed, the C- (C_m-) complexity undergoes a drastic transition, depending on the rate at which measurements are applied, between a regime where it saturates quickly and a regime in which it increases at least linearly until saturating to a values exponentially in the number of qubits. Our conclusions follow from rigorous mathematical arguments which do not rely on any complexity-theoretic assumptions.

We expect our results to extend beyond the brick-wall circuit layout of Fig. 1 to more general circuit architectures. Given any circuit layout, the percolation properties of the corresponding graph is expected to determine the complexity phase transition of the corresponding monitored circuit. Our results are also anticipated to extend beyond the measurement model considered in our work, where measurements in the computational basis occur probabilistically.

The complexity measure C_m we discuss here is defined with respect to a computational model that naturally reflects our setting, by accommodating post-selective measurements alongside unitary gates. A measurement outcome can be post-selected to a desired one if there is non-zero probability with which we obtain the outcome without post-selection. Such state transformation with non-zero probability has been also discussed in the context of the state conversion by stochastic local operations and classical communication (SLOCC) [73, 74]. Also, this computational model is more powerful than the computational model without post-selective measurements [69]; the measure of complexity C_m is thus a lower bound on the usual unitary circuit complexity. Our result therefore indicates that the accessible dimension is a powerful mathematical tool that can also enable us to prove linear growth of such a stronger notion of complexity, the C_m-complexity.

Lemma 7 provides additional insight into the added computational power offered by measurements in monitored quantum circuits. It suggests that while the addition of mea-

surements can enhance the computational power of circuits (e.g., to prepare topologically ordered states [75–78] using constant depth quantum circuits, which is impossible without measurements) they do not explore a set of operations that is larger when measured in terms of accessible dimension. As such, our work offers an approach to quantify the resourcefulness of measurements when tasked with preparing a target state on n qubits.

It is natural to consider other definitions of state complexity, such as some approximate notion of state complexity, the strong complexity [5], the complexity entropy [17], and the spread complexity [79]. The strong complexity, loosely defined as the circuit size required to successfully distinguish a state from the maximally mixed state, displays a markedly different behavior than the C-complexity in monitored random circuits. This behavior is due to the strong complexity being sensitive to the measurement of even a single qubit. Indeed, for any measurement rate p, the presence of a single measurement on an output qubit resets that qubit to the state vector $|0\rangle$, ensuring that the output state is distinguishable from the maximally mixed state. The strong complexity, therefore, saturates quickly for any measurement rate in the large system size limit. This argument furthermore rules out the possibility of monitored random quantum circuits forming a *state t-design* [27] (or complex spherical t-design), since forming a t-design implies reaching a large strong complexity [5]. Moreover, our arguments agree with a recent numerical analysis indicating the absence of a measurement-induced phase transition in monitored random circuits when judged according to the extent the monitored random circuit approximates a t-design; the latter statement has been judged based on the results of an application of a machine learning algorithm [80].

To make robust statements about complexity growth, one would need to smooth the complexity measures $C(|\psi\rangle)$ and $C_m(|\psi\rangle)$ by minimizing the corresponding complexity measure over all states that are ϵ-close to $|\psi\rangle$ in some reasonable metric. Evidence points to a robust version of quantum complexity indeed growing linearly in random circuits: arguments based on k-designs prove robust sublinear growth [5], and variants of this method yield increasingly better properties towards robustness [81]. Proving a similar robustness property of our results appears challenging. It is unclear, for instance, whether arguments based on k-designs can be adapted to circuits with measurements in the general setting. We discuss this point furthermore in Appendix E. In fact, there is growing evidence that states output by a monitored quantum circuit should have efficient representations even in some region below p_c (in the C-complex phase). Indeed, numerical and analytical results [47] highlight an area law behavior of the Rényi-α entropies for $\alpha < 1$ above $p \approx 0.2$–0.35, implying that such states have an efficient representation in terms of MPS [48, 82]. In this regime, a robust definition of state complexity would not exceed $\mathrm{poly}(n)$. It remains an open problem to establish the size of the gap between robust and exact complexity measures in this regime, as well as to determine the precise threshold at which a robust definition of complexity grows linearly until exponential times.

Any region with $p < p_c$ where the monitored circuit's output state would nevertheless obey an area law would provide more concrete examples of states that are naturally described by a circuit but which have shortcuts. Finding shorter circuits that implement a given circuit is usually hard. The regime $p < p_c$ is also one where we might not expect measurements to percolate across the circuit, possibly ruling out the obvious shortcut that corresponds to the original monitored circuit simply resetting the state to a product state at some point during its evolution. This behavior contrasts starkly with random circuits without measurements, where such shortcuts are not expected to occur with any significant probability [5, 13, 81].

We discuss briefly the implication of our result on the AdS/CFT correspondence in

the context of holography. The "complexity=volume conjecture" [12] suggests that the complexity of a CFT state corresponds to the volume of a wormhole in the dual AdS space. Under the assumption that a random circuit can be regarded as a reasonable proxy to study quantum chaotic CFT dynamics, one may argue that monitored random circuits can be seen as proxies of CFT dynamics with local measurements [83–85]. Therefore, in a simplified model where the CFT dynamics is represented by a random circuit with measurements, our results suggest that the volume of a wormhole in the AdS space also undergoes a phase transition by changing the holographic dual of the measurement rate.

This work invites a number of future research directions. First, it would be interesting to study the critical behaviour of the accessible dimension in the monitored circuit in the vicinity of the critical point. It would then be interesting to investigate if the critical exponent of the accessible dimension agrees with that of entanglement entropy [46]. Second, one could give a better lower-bound of the C-complexity in the complex phase. The post-selected measurements can increase the computational power of quantum computers [69]. Similarly, we might expect that measurements could increase the state complexity, which might grow faster than linearly in time. Recently, it has been shown in Ref. [86] that the entanglement velocity—referring to the velocity at which a pair of well-separated regions can become entangled in time—in a monitored circuit below a critical measurement rate with the maximally mixed initial state is larger than that of unitary circuits. It would be interesting to ask if the state complexity grows super-linearly as well in monitored circuits at low measurement rate. Finally, important future directions of research would address the growth of a robust measure of quantum complexity in random monitored circuits as well as in a monitored continuous-time evolution [61–65] In particular, recent proof techniques of Ref. [81] based on the Fourier analysis of Boolean functions appear promising to address these objectives. It may also help to use the analogy of random circuits with the evolution under time-fluctuating Hamiltonians [87] to establish a result of this type: After all, the latter–just like random circuits–give rise to approximate unitary designs with high probability as time goes on. Overall, our work offers new insights on monitored quantum circuits, in which unitary dynamics and measurements are combined together, through the lens of quantum complexity.

6 Acknowledgements

The authors would like to thank Keisuke Fujii and Michael Gullans for useful discussions on monitored quantum circuits, as well as Tomohiro Yamazaki and Sumeet Khatri for useful feedback on an earlier version of this manuscript. We would like to thank the DFG (CRC 183, FOR 2724), the Einstein Foundation (Einstein Research Unit on Quantum Devices), Berlin Quantum, and the FQXi for support. We acknowledge support by the Open Access Publication Fund of Freie Universität Berlin.

A Accessible dimension from algebraic geometry

This section reviews the original definition of the accessible dimension based on semi-algebraic geometry and the results of Ref. [6] and discusses their extensions to monitored random quantum circuits in order to establish Lemma 4. The facts from algebraic geometry and differential geometry and lemmas here follow the corresponding statements in the Appendix of Ref. [6], where there are more detailed references. A key observation there is that the set of the all output states $\mathcal{S}^A$ forms a semi-algebraic set, and its "dimension" can be meaningfully defined and bounded, although it is neither a vector space nor a manifold.

First, we introduce some basic notions of algebraic geometry. A subset $V \subseteq \mathbb{R}^m$ is called an *algebraic set*, if for a set of polynomial maps $\{f_j\}_j$,

$$V = \{x \in \mathbb{R}^m | f_j(x) = 0 \text{ for all } j\}. \tag{20}$$

Also, we call a subset $W \subseteq \mathbb{R}^m$ a *semi-algebraic set*, if for sets of polynomial maps $\{f_j\}_j$ and $\{g_k\}_k$,

$$W = \{x \in \mathbb{R}^m | f_j(x) = 0,\ g_k(x) \leq 0 \text{ for all } j \text{ and } k\}. \tag{21}$$

The following observation is an immediate consequence of the *Tarski-Seidenberg principle*, which states that for a polynomial map F and a semi-algebraic set W, $F(W)$ is again a semi-algebraic set.

Observation 11 (The set of output states is semi-algebraic)**.** *$\mathcal{S}^M$ is a semi-algebraic set.*

Proof. A set $[\mathrm{SU}(4)]^{\times R}$ is an algebraic set, because it is the set of operators whose matrix elements satisfy polynomial equations equivalent to $U^\dagger U = I$ and $\det U = 1$. Besides, the contraction map F^M is a polynomial map, that is, the map to output states is a polynomial function of matrix elements of $\{U_j\}_{j=1}^R$. Therefore, by the Tarski-Seidenberg principle, we arrive at the stated observation. □

In a next step, we introduce a notion of a dimension for a semi-algebraic set. It originates from the fact that all semi-algebraic sets can be decomposed into a set of smooth manifolds.

Fact 1 (Semi-algebraic sets and smooth manifolds)**.** *For a semi-algebraic set W, there exist a set of smooth manifolds $\{N_j\}_j$ such that $W = \bigcup_j N_j$. Moreover, $\max_j\{\dim(N_j)\}$ does not depend on the decomposition of W.*

Definition 12 (Dimension of semi-algebraic sets)**.** *For a semi-algebraic set W, with decomposition into smooth manifolds $W = \bigcup_j N_j$, the dimension of W is defined as $d := \max_j\{\dim(N_j)\}$.*

Using the same argument as in Lemma 1 in Ref. [6], one can show that the above dimension of $\mathcal{S}^M$ is equal to the accessible dimension laid out in Definition 3.

Lemma 13 (Equivalence of two definitions of dimension)**.** *Let $\dim \mathcal{S}^M$ be the dimension of the semi-algebraic set $\mathcal{S}^M$, defined by Definition 12. Then $\dim \mathcal{S}^M$ is equal to the accessible dimension d_M, defined by Definition 3.*

Then, we prove Lemma 4.

Lemma 14 (Restatement of Lemma 4)**.** *If $d_M \geq k$ for an integer k, then*

$$C(|\psi\rangle) \geq \frac{1}{11}\left(k - 3n - 2\right), \tag{22}$$

$|\psi\rangle \in \mathcal{S}^A$, with unit probability, that is, for almost all unitary gates.

Proof. The proof goes similarly to that of Theorem 1 in Ref. [6], and we refer to that reference for further details. The only difference with the argument presented there is that the shorter circuit in Ref. [6] becomes a post-selected quantum circuit and the state vectors in $\mathcal{S}^M$ are not normalized in general. The latter means that unitary gates are realized with the probability specified by the Born rule $\langle 0^n|V^M(t)^\dagger V^M(t)|0^n\rangle \prod_{i=1}^R d\mu_{\mathrm{Haar}}(U_i)$, where $d\mu_{\mathrm{Haar}}$ is the Haar measure on SU(4). The strategy is to show that for $\mathcal{S}^M$ with $d_M \geq k$,

the set of states in $\mathcal{S}^M$ generated by a unitary circuit with R' two-qubit gates, which is less than $(k-n-2)/13$, is measure zero. We explain it in more detail below.

Let $\mathcal{S}'$ be the set of the all unnormalized output state vectors of a short post-selected quantum circuit consisting of R' two-qubit unitary gates with an arbitrary architecture and measurement configuration. Then, $\mathcal{S}'$ is also a semi-algebraic set. Recall that the accessible dimension of S', d', is the number of linearly independent vectors of

$$\{F^M(U_1,\ldots,(\alpha\otimes\beta)U_j,\ldots,U_R)\}_{j,\alpha,\beta}, \tag{23}$$

where $j\in\{1,2,\ldots,R'\}$ and $\alpha,\ \beta\in\{I,X,Y,Z\}$ are Pauli operators such that $(\alpha,\beta)\neq(I,I)$. The number of state vectors in Eq. (23) is at most $15R'$, and we find that $\dim(\mathcal{S}')\leq 15R'$. We can improve the upper-bound to $11R'+3n$, by considering the contraction of two-qubit gates $U_{i-1,i}$, acting on qubits $i-1$ and i, followed by $U_{i,i+1}$ that shares a bond of the gates, that is i-th qubit. Indeed, if there is no measurement on qubit i just after $U_{i-1,i}$, the state vector in Eq. (23) generated by contracting the perturbed $U_{i-1,i}$, $(I\otimes\alpha)U_{i-1,i}$, and other two-qubit gates is equal to the vector generated by contracting $U_{i,i+1}(\alpha\otimes I)$ and others for any non-identity Pauli operator α. It means that 3×2 parameters are redundant for each two-qubit gate in a circuit's bulk. For the first $\frac{n}{2}$ gates, the parameters are not cancelled, and so are not $3n$ parameters. Similarly if there is a projector on qubit i, the perturbations of $(I\otimes Z)U_{i-1,i}$ and $U_{i,i+1}(Z\otimes I)$ result in the same vector, and also the perturbations of $(I\otimes X)U_{i-1,i}$ and $(I\otimes Y)U_{i-1,i}$ result in vectors linearly dependent with each other. It means that 2×2 parameters are redundant in this case. Therefore, we obtain

$$\begin{aligned}\dim(\mathcal{S}') &\leq 15R'-3(2R'-m)-2m+3n \\ &= 9R'+m+3n \\ &\leq 11R'+3n,\end{aligned} \tag{24}$$

where m is the number of measurements in the post-selected circuit, and we used $0\leq m\leq 2R'$ in the last inequality.

A quantum state vector $|\psi\rangle\in\mathcal{S}^M$ is generated by a short post-selected quantum circuit if there exists a $|\phi\rangle\in\mathcal{S}'$ such that $|\psi\rangle=c\,|\phi\rangle$ for some $c\in\mathbb{C}$. We show that the set of such state vectors

$$\{|\psi\rangle\in\mathcal{S}^M|\,|\psi\rangle=c\,|\phi\rangle\,,\ \text{for}\ \ |\phi\rangle\in\mathcal{S}',c\in\mathbb{C}\} \tag{25}$$

is of measure zero in $\mathcal{S}^M$, and so its preimage by F^A in $SU(4)^R$ is. By Fact 1, the set of the elements of $\mathcal{S}'$ multiplied by arbitrary complex numbers, can be decomposed into smooth manifolds. Then, the maximal dimension of them is upper bounded by $11R'+3n+2$, because complex coefficients add at most two real parameters. Then, if $R'<(k-3n-2)/11$, d_M is greater the dimension of the maximal manifold. Therefore, the intersection $\{|\psi\rangle\in\mathcal{S}^M|\,|\psi\rangle=c\,|\phi\rangle\,,\ \text{for}\ \ |\phi\rangle\in\mathcal{S}',c\in\mathbb{C}\}$ has Haar measure zero, because the manifolds in $\mathcal{S}'$ multiplied by arbitrary complex numbers have smaller dimensions than the maximal dimension of that in S^M. This implies that the set of unitary gates in $SU(4)^{R'}$, with $R'<(k-3n-2)/11$, that generate states in the intersection is also Haar measure zero [6]. Because $\langle 0^n|V^M(t)^\dagger V^M(t)|0^n\rangle$ is upper-bounded by finite value, that is 1, it is still measure zero for the product measure of the Haar measure and the Born probability, that is $\langle 0^n|V^M(t)^\dagger V^M(t)|0^n\rangle\prod_{i=1}^R d\mu_{\mathrm{Haar}}(U_i)$. Therefore, the output states of the monitored circuit with the dimension k cannot be generated by shorter quantum circuits consisting of fewer than $(k-3n-2)/11$ gates with unit probability, which implies the desired lower-bound of the state complexity. □

Finally, we prove Lemma 10. We have considered a lower-bound for the accessible dimension of unitary circuits $d_0(t)$, with the brick-wall architecture and with depth t, consisting of the following random unitary gates:

$$U = (u_1 \otimes v_1)\, W\, (u_2 \otimes v_2)\,, \tag{26}$$

where $u_{1,2}$, $v_{1,2}$ are Haar-random single-qubit gates and W is chosen from $\{I,\ \mathrm{CNOT}\}$ uniformly randomly.

Lemma 15 (Restatement of Lemma 10)**.** *Let $t \geq 0$ be an integer. Then, d_0 grows linearly in depth t as*

$$d_0(t) \geq \left\lfloor \frac{2t}{3n} \right\rfloor, \tag{27}$$

until it saturates in a depth exponential in n.

Proof. Recall that d_0 is the maximum dimension of the following vector space over unitary gates $\{U_1, U_2, \ldots, U_R\}$ in the form of Eq. (26),

$$\{U_R \ldots (\alpha \otimes \beta) U_j \ldots U_1 \left|0^n\right\rangle)\}_{j,\alpha,\beta}, \tag{28}$$

where $(\alpha \otimes \beta)$ is a single-qubit perturbation: $(\alpha, \beta) = (I, \sigma), (\sigma, I)$ for $\sigma \in \{X, Y, Z\}$. In Ref. [6], a unitary circuit consisting of Clifford gates is constructed in which d_0 grows linearly in depth. The strategy there is to construct a Clifford circuit inductively such that a linear number in t of vectors

$$P_{\alpha,\beta,j} \left|0^n\right\rangle \in \{i^\kappa \left|x\right\rangle\}_{x\in\{0,1\}^n, \kappa\in\{0,1\}}, \tag{29}$$

where $P_{\alpha,\beta,j} = U_1^\dagger \ldots U_j^\dagger (\alpha \otimes \beta) U_j \ldots U_1$, are linearly independent. We define C_j as a depth-$n/2$ Clifford circuit with arbitrary Clifford two-qubit gates. In particular, there is a Clifford circuit such that the vectors

$$\{C_1^\dagger \ldots C_j^\dagger (Z \otimes I) C_j \ldots C_1 \left|0^n\right\rangle\}_{j=1}^T, \tag{30}$$

where $T = \lfloor \frac{2t}{n} \rfloor$, are linearly independent because of the observation that a depth-$\frac{n}{2}$ Clifford circuit is enough to turn $Z \otimes I$ into an arbitrary Pauli string by conjugating it [6]. Moreover, each two-qubit Clifford gate can be decomposed into at most three CNOT gates with single-qubit gates [88]. Therefore, every $\frac{3n}{2}$ time step can increase the accessible dimension at least by one, and we obtain

$$d_0(t) \geq \left\lfloor \frac{2t}{3n} \right\rfloor. \tag{31}$$

□

The dimension d_0 is upper-bounded by $2\times 2^n - 1$, which is the number of real parameters in normalized quantum states, and it grows linearly until it saturates at the maximum value exponentially in n.

B Measurements cannot increase the accessible dimension

In this section, we prove that the accessible dimension of a monitored random circuit cannot increase by adding a projection operator. Let M be a measurement configuration. We now construct a new measurement configuration M' by changing an element $M_i(\tau)$ such that $M_i(\tau) = \sqrt{1-p}I$ into $M_i'(\tau) = \sqrt{p}\,|0\rangle\langle 0|$ or $M_i'(\tau) = \sqrt{p}\,|1\rangle\langle 1|$ and keeping the other elements. We denote by $|M|$ the number of projections in M, and hereafter we rename the set of projectors as $\{M_i\}_{i=1}^{|M|}$. We call such M_i' the additional measurement. Then the following statement holds.

Lemma 16 (Rank bound)**.** *For* $\mathrm{rank}(F^{M'})$ *on an arbitrary point* $x' \in SU(4)^{\times R}$*, there exists a point* $x \in SU(4)^{\times R}$*, on which* $\mathrm{rank}(F^{M})$ *satisfies the inequality:*

$$\mathrm{rank}(F^{M'}) \leq \mathrm{rank}(F^{M}). \tag{32}$$

Proof. We fix R gates mapped by $F^{M'}$ as $x' = \{U_R, \ldots, U_1\}$. By definition, the rank r' of $F^{M'}$ is

$$r' = \dim\left(\mathrm{span}\left\{U_R \cdots M'_{|M'|} \cdots M'_k U_m \cdots (\alpha \otimes \beta) U_j \cdots M'_1 \cdots U_1 \,|0^n\rangle\right\}_{j,\alpha,\beta}\right), \tag{33}$$

where M_k' is the additional measurement $M_k' = \sqrt{p}\,|0\rangle\langle 0|$ (we assume here that the outcome of M_k is $+1$, but the case of -1 works as well). Because of $|0\rangle\langle 0| = (I+Z)/2$, Eq. (33) becomes

$$r' = \dim\left(\mathrm{span}\left\{U_R \cdots M'_{|M'|} \cdots (I+Z) U_m \cdots (\alpha \otimes \beta) U_j \cdots M'_1 \cdots U_1 \,|0^n\rangle\right\}_{j,\alpha,\beta}\right), \tag{34}$$

where U_m is the unitary gate which is just followed by the measurement M_k. By the definition of dimension, there are r' linearly independent vectors $|v_i\rangle := U_R \cdots M_{|M|} \cdots (I + Z)U_m \cdots (\alpha \otimes \beta)U_j \cdots M_1 \cdots U_1 \,|0^n\rangle$, $i = 1, \ldots, r$, where the index i denotes the configuration of α, β, and j.

Now, we set x as the same as x' except for m-th gate, which is $e^{i(I+Z)\theta}U_m$. Then, $\mathrm{rank}(F^M)$ is the dimension of the vector space spanned by the vectors

$$\left\{U_R \cdots M_{|M|} \cdots e^{i(I+Z)\theta} U_m \cdots (\alpha \otimes \beta) U_j \cdots U_1 \,|0^n\rangle\right\}_{j,\alpha,\beta}, \tag{35}$$

which are equal to

$$\begin{aligned}&\Big\{U_R \cdots M_{|M|} \cdots U_m \cdots (\alpha \otimes \beta) U_j \cdots M_1 \cdots U_1 \,|0^n\rangle \\ &\quad + U_R \cdots M_{|M|} \cdots (e^{i\theta} - 1)(I+Z) U_m \cdots (\alpha \otimes \beta) U_j \cdots M_1 \cdots U_1 \,|0^n\rangle\Big\}_{j,\alpha,\beta}.\end{aligned} \tag{36}$$

Using the vectors $\{|v_i\rangle\}$, we can find r independent vectors in Eq. (36). Specifically, we can find some θ such that the r vectors

$$\begin{aligned}&|u_i\rangle + (e^{i\theta} - 1)\,|v_i\rangle \\ &= U_R \cdots M_{|M|} \cdots U_m \cdots (\alpha \otimes \beta) U_j \cdots M_1 \cdots U_1 \,|0^n\rangle \\ &+ (e^{i\theta} - 1) U_R \cdots M_{|M|} \cdots (I+Z) U_m \cdots (\alpha \otimes \beta) U_j \cdots M_1 \cdots U_1 \,|0^n\rangle\end{aligned} \tag{37}$$

are linearly independent for $i = 1, \ldots, r$, where we have defined $|u_i\rangle$ and $(e^{i\theta} - 1)\,|v_i\rangle$ as the first term and the second term of the right-hand side of the equation, respectively.

To see this, first, we make r orthonormal vectors $\{|\tilde{v}_i\rangle\}$ from $\{|v_i\rangle\}$ by the Gram-Schmidt decomposition. By these vectors, $\{|v_i\rangle\}$ is decomposed as $|v_i\rangle = \sum_{k=1}^{i} d_i^k |\tilde{v}_k\rangle$, for some coefficients d_i^k such that $d_i^i \neq 0$ for all i. Next, decompose $|u_i\rangle$ as

$$|u_i\rangle = \sum_{k=1}^{r} c_i^k |\tilde{v}_k\rangle + c_i^\perp \left|v_i^\perp\right\rangle, \tag{38}$$

for some coefficients c_i^k, $c_i^\perp$ and some vector $\left|v_i^\perp\right\rangle$ in the orthogonal complement of $\mathrm{span}\{|v_i\rangle\}$. Let us define the function $f : \mathbb{R} \to \mathbb{C}$ as

$$f(\theta) := e^{i\theta} - 1. \tag{39}$$

Then, Eq. (37) becomes

$$\sum_{k\leq i} (c_i^k + f(\theta) d_i^k) |\tilde{v}_k\rangle + \sum_{k>i} c_i^k |\tilde{v}_k\rangle + c^\perp \left|v_i^\perp\right\rangle. \tag{40}$$

Again, we make r orthonormal vectors $\{\left|\tilde{v}_i^\perp\right\rangle\}$ from $\{\left|v^\perp{}_i\right\rangle\}$ by the Gram-Schmidt decomposition, and $\left|v^\perp{}_i\right\rangle = \sum_{k=1}^{i} e_i^k \left|\tilde{v}_k^\perp\right\rangle$ for some coeffients e_i^k. Consider a linear map A, which maps $|\tilde{v}_i\rangle$ to Eq. (40). In the matrix representation with the basis $\{|\tilde{v}_i\rangle, \left|\tilde{v}_i^\perp\right\rangle\}_{i=1,\ldots,r}$,

$$A = \begin{pmatrix} c_1^1 + f(\theta)d_1^1 & c_2^1 + f(\theta)d_2^1 & \cdots & c_r^1 + f(\theta)d_r^1 \\ c_1^2 & c_2^2 + f(\theta)d_2^2 & \cdots & c_r^2 + f(\theta)d_r^2 \\ \vdots & \vdots & \ddots & \vdots \\ c_1^r & c_2^r & \cdots & c_r^r + f(\theta)d_r^r \\ e_1^1 & e_2^1 & \cdots & e_r^1 \\ 0 & e_2^2 & \cdots & e_r^2 \\ \vdots & \vdots & \ddots & \vdots \\ 0 & 0 & \cdots & e_r^r \end{pmatrix}, \tag{41}$$

where it is an $2r \times r$ matrix. Let $A^{r\times r}$ be the top $r \times r$ sub-matrix of A. Note that if the $\mathrm{rank}(A^{r\times r}) = r$, then $\mathrm{rank}(A) = r$, and it implies that the vectors $\{|u_i\rangle + (e^{i\theta} - 1)|v_i\rangle\}_{i=1,\ldots,r}\}$ are linearly independent. This condition is equivalent to that $A^{r\times r}$ has a non-zero determinant. Moreover, we can always choose θ such that $\mathrm{rank}(A^{r\times r}) = r$. This is because the determinant of $A^{r\times r}$ is a polynomial of $F(\theta)$ such that its zeros imply $\mathrm{rank}(A^{r\times r}) < r$, and by virtue of the fundamental theorem of algebra, the number of zeros of the polynomial is the same as its degree, which is r. We can choose θ such that it is not any zeros of the polynomials, because θ is a continuous variable. Hence, such θ gives $\mathrm{rank}(F^M)$ which is greater than or equal to $\mathrm{rank}(F^{M'})$. □

Because the accessible dimension is the maximal rank over R unitary gates, the above lemma implies that single-qubit measurement, or projection, cannot increase the accessible dimension. Applying the above lemma recursively, we can show that adding any number and space-time point of measurements cannot increase the dimension.

C Two-qubit gate between nearest-neighbour measurement-free paths

In this section, we show how unitary gates at the edge of the bridge are fixed to implement a CNOT gate between two neraest-neighbour measurement-free paths. For completeness,

we begin with restating the method in the main text, where we consider the following paths and bridge,

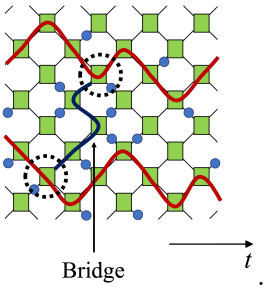

(42)

Then, CNOT can be implemented as Eq. (18), and we restate it here as

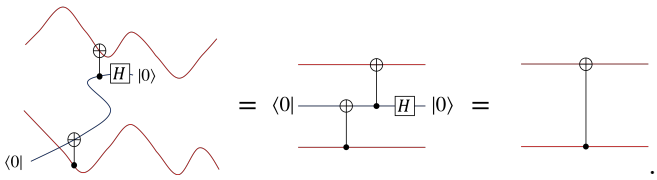

(43)

In this case, both of the paths in Eq. (42) are causal in the broken circles, that is, they include both an input and an output of the unitary gates in the circles. In general, in such case we can perform CNOT, by applying a CNOT gate, multiplied by $I \otimes H$, with the control qubit being measured and another CNOT gate with the target qubit state being measured at the edge of the bridge, such as Eq. (43).

If this is not the case, we can still implement a CNOT gate, as we explain below. We consider the case where one path is causal, and another path is not causal at the edge of a bridge, for example

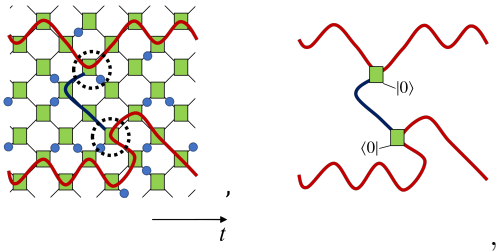

(44)

where in the right-hand side, we highlighted the paths, the bridge, and two-qubit gates at the edge of the bridge. We can also perform CNOT in such case, by applying a CNOT gate, multiplied by $I \otimes H$, with the control qubit state being measured and another CNOT gate with the target qubit state being measured. For the above example, it is performed as the following:

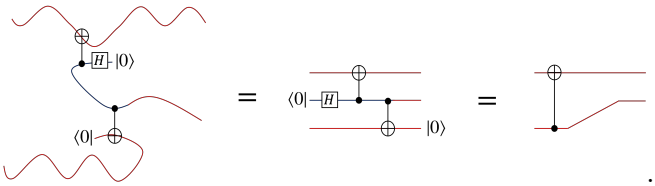

(45)

The difference with the earlier case is that here the qubit state carried by a bridge is an output state of one measurement-free path. Finally, we consider the case where both of

the paths are not causal at the edge of a bridge, for example

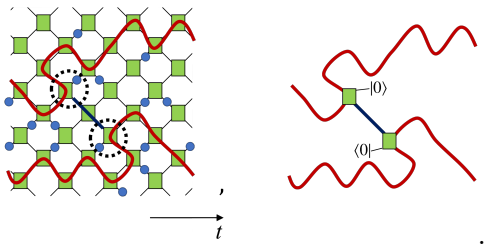

(46)

Again, we can perform CNOT in such case, by a similar choice of two-qubit gates at the edge of the bridge. For the above example,

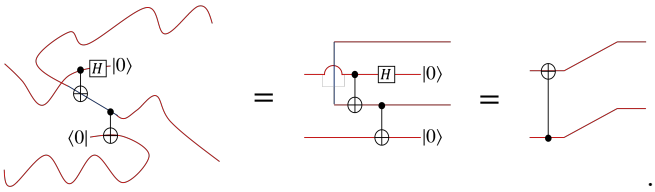

(47)

D Percolation theory

In this work, techniques from percolation theory feature strongly. For this reason, here we review some aspects of percolation theory, following Ref. [68], and then prove lemmas used in the main text. Specifically, we focus on the percolation theory on a rectangle featuring a large aspect ratio.

Especially important are notions of *bond percolation* on two-dimensional square lattices. A square lattice is defined as $\mathbb{Z}^2$ with edges between all nearest-neighbor pairs $x, y \in \mathbb{Z}^2$. We denote by $\mathbb{E}$ the set of *edges*. We define a measurable space $(\Omega, \mathcal{F})$ as follows. For the sample space, we take $\Omega = \prod_{e\in\mathbb{E}}\{0,1\}$, called the edge configuration (0 and 1 represent closed and open edge, respectively), and $\mathcal{F}$ is the σ-algebra on it. Each element in Ω is represented as a function $\omega : \mathbb{E} \to \{0,1\}$. We say $\omega \leq \omega'$ if $\omega(e) \leq \omega'(e)$ for all $e \in \mathbb{E}$. Let $A \in \mathcal{F}$ be an *increasing event*, i.e.,

$$I_A(\omega) \leq I_A(\omega') \tag{48}$$

whenever $\omega \leq \omega', \omega, \omega' \in \Omega$. Here, $I_A : \Omega \to \{0,1\}$ is the *indicator function* of A: $I_A(\omega) = 1$ if $\omega \in A$ and otherwise $I_A(\omega) = 0$. For an event A, we denote the probability of the occurrence of the event by $P_q(A)$ when an edge opens with probability q. (This q is contrary to that in the section 2.1. There, a measurement closes, or "cut" a bond, at probability "p" but in this section, bond is open at probability q.) For two increasing events A and B, the inequality

$$P_q(A \cap B) \geq P_q(A)P_q(B) \tag{49}$$

is well known as the *FKG inequality* in the literature of percolation theory. Intuitively, the FKG inequality tells us that if we know an increasing event A occurs, another increasing event B is more or equally likely to occur.

Bond percolation theory is concerned with the existence or absence of *left-right crossings* on a $L \times L$ square, which is an open path connecting from some vertex on the left side of the square to the right side of it. With probability exponentially close to one in L, above the critical probability q_c, there exists such crossings, and below it, there does

not. Moreover, the critical point of bond percolation in two-dimensional square lattice is known to be $q_c = 1/2$ [68]. In the following subsections, we show several lemmas to establish Theorem 5.

D.1 Supercritical phase

A main goal here is to derive a lower-bound of the expected number of left-right crossings on a rectangle with a various aspect ratio in the regime $q > q_c = \frac{1}{2}$.

D.1.1 Percolation on a square

We start the argument by discussing the case of a square. Let M_L be the maximal number of edge-disjoint left-right crossings of the box $[0, L] \times [0, L]$ for an integer L. In this appendix, we use the shorthand $[0, a] \times [0, b]$ to designate the rectangular lattice of points of height a and width b. In the supercritical phase the probability of the event A, where there exists an left-right crossing in the box $[0, L] \times [0, L]$, is exponentially close to one [68]:

$$P_q(A) \geq 1 - e^{-\alpha L}, \tag{50}$$

for some constant $\alpha = \alpha(q)$. The event A is an increasing event, because adding open edges does not decrease the number of left-right crossings.

Now we define the *interior* of A, $J_r(A)$, as the set of configurations in A which are still in A after changing arbitrarily the configurations at most r edges (deleting or adding edges). The following fact states the stability of an increasing event.

Fact 2 (Theorem 2.45 in Ref. [68])**.** *Let A be an increasing event. Then*

$$1 - P_{q_2}(J_r(A)) \leq \left(\frac{q_2}{q_2 - q_1}\right)^r (1 - P_{q_1}(A)) \tag{51}$$

for any $0 \leq q_1 < q_2 \leq 1$.

Roughly speaking, it states that if the event A happens with probability q_1, the modified event J_r is also likely to happen when probability exceeds q_1. The above fact is useful for finding a lower-bound of the number of crossings of a rectangle. $J_r(A)$ is the events that there exists at least $r + 1$ left-right crossing (because if there are less than $r + 1$ crossings, deleting r edges can cut all the crossings). Combining Eq. 50 with Fact 2, the following statement is obtained.

Fact 3 (Lemma 11.22 in Ref. [68])**.** *For $q > 1/2$, there exists strictly positive constants $\beta(q)$ and $\gamma(q)$, which are independent in n, such that $P_q(M_L \geq \beta(q)L) \geq 1 - e^{-\gamma(q)L}$ for all $L \geq 1$.*

Proof. One starts by choosing r in Fact 2 as $\beta(q)L$, and the set A as being the event that there exists at least one left-right crossing. Then Fact 2 implies

$$1 - e^{-L\left(\alpha(q') - \beta(q) \log \frac{q}{q - q'}\right)} \leq P_q(M_{n+1} \geq \beta(q)L), \tag{52}$$

where $q > q' > 1/2$. Now we find

$$\gamma(q) = \alpha(q') - \beta(q) \log \frac{q}{q - q'}. \tag{53}$$

For a fixed $1 \geq q > \frac{1}{2}$, we can choose a strictly positive constant $\beta(q)$ and q' such that $\gamma(q)$ is also strictly positive. □

The above statement implies that if a left-right crossing exists at a high probability in a square lattice, we can find a number of edge-disjoint left-right crossings, which scale in the length of the side of a square, at a high probability. It ensures the existence of a linear number of measurement-free paths. We mention that Refs. [89–91] have made a similar use of Facts 2 and 3 as well in the context of the measurement-based quantum computation.

D.1.2 Percolation on a rectangle with a various aspect ratio

Next we consider a square lattice on a rectangle $[0, L] \times [0, LT]$ for some aspect ratio $T > 1$. We can show the existence of a scalable number of left-right crossings until some exponential aspect ratio. It is true in the case of both bond and site percolation. We make use of following facts. Let A_T be an event that there exists a right-left crossing on $[0, L] \times [0, LT]$ rectangle.

Fact 4 (Lemma 11.73 and 11.75 in Ref. [68])**.** *If* $P_q(A_1) = \tau$*, then*

$$P_q\left(A_{\frac{3}{2}}\right) \geq (1 - \sqrt{1-\tau})^3, \tag{54}$$

$$P_q(A_2) \geq P_q(A_1) P_q\left(A_{\frac{3}{2}}\right). \tag{55}$$

These insights (*FKG inequality*) assist us in proving the following lemma.

Lemma 17 (Large aspect ratios)**.** *If* $P_q(A_1) = \tau$*, then*

$$\begin{aligned} P_q(A_T) &\geq P_q(A_1)^{T-2} P_q\left(A_2\right)^{T-1} \\ &\geq \tau^{2T-3} (1 - \sqrt{1-\tau})^{3(T-1)}. \end{aligned} \tag{56}$$

Proof. To start with, note that if there are top-bottom crossings in every square except for both ends and left-right crossings in every nearest-neighbor two squares, then there exists at least one left-right crossing over the entire rectangle, or, graphically,

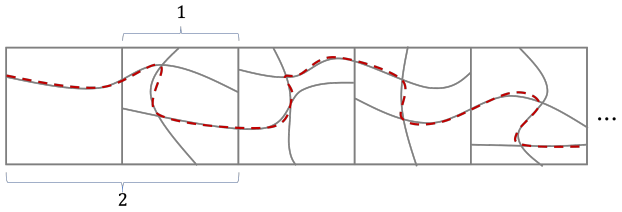

,

where the broken line is the left-right crossing over the rectangle. Besides,

$$\left(\bigcap_{i=1}^{T-2} A_1\right) \bigcap \left(\bigcap_{i=1}^{T-2} A_2\right) \subset A_T, \tag{57}$$

and it can be straightforwardly shown that A_1 and A_2 are increasing events. Hence, by the FKG inequality, the inequality Eq. (56) holds, and together with Fact 4, we arrive at the validity of the second inequality as well. □

From the above lemma together with Fact 2, we can guarantee a linear number of edge-disjoint left-right crossings. Let M_L^T be the maximal number of edge-disjoint open left-right crossings of the box $[0, L] \times [0, LT]$.

Lemma 18 (Linear paths)**.** *For $q > 1/2$, there exists strictly positive constants $\beta(q)$ and $\gamma(q)$, which are independent of n, such that*

$$P_p(M_L^T \geq \beta(q)L) \geq 1 - e^{-\gamma(q)L} \tag{58}$$

for all $L \geq 1$.

Proof. For $q > 1/2$, because of

$$\tau \geq 1 - e^{-\alpha(p)L} \tag{59}$$

and Lemma 17, we obtain

$$\begin{aligned} P_q(A_T) \geq& \left(1 - e^{-\frac{\alpha(q)}{2}L}\right)^{3(T-1)} \times \left(1 - e^{-\alpha(q)L}\right)^{(2T-3)} \\ \geq& \left(1 - e^{-\frac{\alpha(q)}{2}L + \log 3(T-1)}\right) \times \left(1 - e^{-\alpha(q)L + \log(2T-3)}\right) \\ \geq& 1 - e^{-\frac{\alpha(q)}{2}L + \log 3(T-1)} - e^{-\alpha(q)L + \log(2T-3)} \\ \geq& 1 - 2e^{-\frac{\alpha(q)}{2}L + \log 3(T-1)}, \end{aligned}$$

where, in the second inequality, we have used the Bernoulli's inequality

$$(1 + x)^y \geq 1 + xy \tag{60}$$

for any real numbers $x \geq -1, y \geq 1$. Using Fact 2, this implies that the number of left-right crossings scales in the system size. Specifically,

$$P_q(M_L^T \geq \beta(q)L) \geq 1 - e^{-\left(\frac{\alpha(q')}{2} - \beta(q)\log\frac{q}{q-q'}\right)L + \log 6(T-1)} \tag{61}$$

where $q > q' > 1/2$. We find that

$$\gamma(q) = \frac{\alpha(q')}{2} - \beta(q)\log\frac{q}{q-q'} - \frac{1}{L}\log 6(T-1). \tag{62}$$

We can pick a strictly positive constant $\beta(p) > 0$ and $\frac{1}{2} < q' < q$ such that $\gamma(q)$ is also strictly positive. □

This lemma ensures that at below critical measurement probability, there exists a linear number of measurement-free paths until some exponential time. Specifically, if

$$T < \frac{e^{\frac{\gamma'(q)}{2}n}}{3} \tag{63}$$

for some strictly positive

$$\gamma'(q) < \frac{\alpha(q')}{2} - \beta(q)\log\frac{q}{q-q'}, \tag{64}$$

there exists $\lfloor \beta(q)L \rfloor$ left-right crossings on a rectangle almost surely in the large L limit.

D.2 Subcritical phase

Next, we consider the size of a set of connected open edges in the subcritical phase $q < q_c$. The *open cluster* $C(x)$ at a vertex x of the square lattice is defined by the set of the connected open edges containing x, and $|C(x)|$ denotes the number of the edges in $C(x)$. Then, the probability that the size $|C(x)|$ is large is upper bounded as follows.

Fact 5 (Theorem 6.75 in Ref. [68])**.** *Let $C(x)$ be an open cluster containing a vertex x. If $q < q_c = \frac{1}{2}$, there exists $\lambda(q) > 0$ such that for any integer $k \geq 1$,*

$$P_q(|C(x)| \geq k) \leq e^{-k\lambda(q)}. \tag{65}$$

The independence of x in the right-hand side is due to translational invariance of the square lattice. Now, we upper-bound the probability of the event that all size of m open clusters,

$$\{C(x_1), C(x_2), \ldots, C(x_m)\}, \tag{66}$$

is upper-bounded by an integer k, which we define by

$$P_q\left(\bigcup_{i=1}^{m}\{|C(x_i)| \geq k\}\right). \tag{67}$$

Lemma 19 (Small open clusters)**.** *For $q < 1/2$, there exists $\lambda(q) > 0$ such that for any real number $0 < \epsilon < 1$ and any integer $k \geq \frac{1}{\lambda(q)} \log(\frac{m}{\epsilon})$,*

$$P_q\left(\bigcup_{i=1}^{m}\{|C(x_i)| \geq k\}\right) \leq \epsilon. \tag{68}$$

Proof. By the union bound and Fact 5, we obtain

$$P_q\left(\bigcup_{i=1}^{m}\{|C(x_i)| \geq k\}\right) \leq \sum_{i=1}^{m} P_q\left(|C(x_i)| \geq k\right) \tag{69}$$

$$\leq m e^{-k\lambda(q)}. \tag{70}$$

Then, by the condition

$$k \geq \frac{1}{\lambda(q)} \log\left(\frac{m}{\epsilon}\right), \tag{71}$$

we obtain Eq. (68). □

D.3 Tilted lattice and untilted lattice

As shown in Fig. 2 in the main text, a monitored circuit is mapped to a tilted square lattice. In percolation theory, however, bond percolation on a square lattice is ordinarily considered for an untilted square lattice, consisting of horizontal edges. We show how they are related by proving that the critical points of them are same.

We consider bond percolation on an $2n \times 2n$ ordinary square lattice above the critical point, and the $n \times n$ tilted square whose corners are at the middle of the edges of the $2n \times 2n$ square lattice. Then, with probability $1 - e^{-\Omega(n)}$, there exist at least one left-right and one top-bottom crossings in rectangles $[0, \lfloor \frac{n}{2} \rfloor] \times [0, 2n]$ just above the middle horizontal line and right next to the middle vertical line, respectively, or graphically,

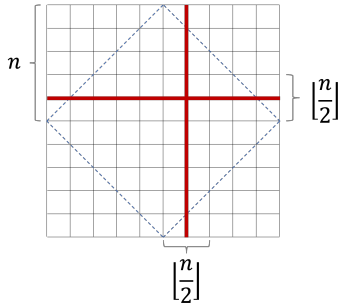

,

where the square with broken lines is the $n \times n$ tilted square, and we assumed the crossings are straight. It implies by the FKG inequality that there exists at least one left-right crossing in the tilted square lattice. Also, one can show conversely that left-right and top-bottom crossings in a $2n \times 2n$ tilted lattice implies a crossing in an $n \times n$ ordinary square lattice inside it by the same argument. Therefore, the critical points of percolation on both lattices are the same.

E Lower bound on approximate complexity

In this section, we give a lower bound on the approximate complexity of some class of output states in monitored random circuits at a small measurement rate.

Definition 20 (C_ϵ approximate complexity)**.** *The ϵ-approximate complexity of a quantum state $|\psi\rangle$, $C_\epsilon(|\psi\rangle)$, is the minimum number of two-qubit gates to generate $|\psi\rangle$ up to an error ϵ in the trace distance from an initial product state. The gates can be any elements of $SU(4)$ and the circuit may have any chosen connectivity.*

To lower-bound the approximate complexity, we again use the percolation argument, which is in Section 4.3. We consider a regime of a small enough measurement rate where there are $\Omega(n)$ causal measurement-free paths and they meet at some space-time points. We also assume that any pair of nearest-neighbour paths meet $\Omega(t)$ time so that we can embed a unitary circuit with the brick-wall architecture and circuit depth $\Omega(t)$. In this embedding, we apply the suitable two-qubit along the paths, for example we applied I, SWAP, and random two-qubit gates at the points they meet, in the broken circles as shown below:

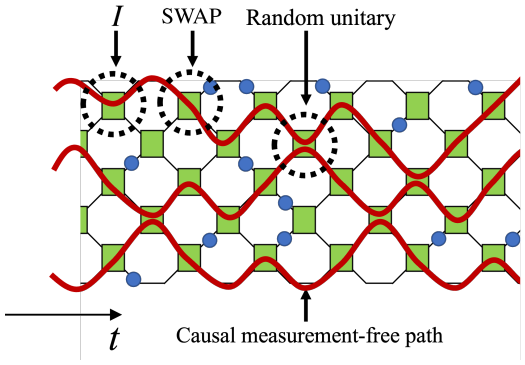

. (72)

Moreover, we fix all unitary gates outside the paths as the identity gate I.

Let S'^M be the set of all normalized output states generated by the monitored circuit with measurement configuration M and initial state $|0^n\rangle$. In the above setting, we can embed $\Omega(t)$-depth random unitary circuit into the monitored circuit, and we have $S'^M =$

$\{|\psi\rangle \otimes |0_{\text{rest}}\rangle\}$, where $|\psi\rangle$ is an output state of $\Omega(n)$-qubit $\Omega(t)$-depth random unitary circuit and $|0_{\text{rest}}\rangle$ is the state outside the measurement-free paths. To lower-bound on the C_ϵ-complexity of $|\psi\rangle \otimes |0_{\text{rest}}\rangle$, we use the bound on the C_ϵ-complexity of random unitary circuits as the following. The output states of random unitary circuits with the brick-wall architecture, the circuit depth t, and an initial pure state form the approximate state k-design in $O(nk^{5+o(1)})$-depth with an approximation error constant in n [92]. Moreover, for ϵ which is constant in n, the states from the approximate state k-design have at least $\Omega(k)$ C_ϵ-complexity at probability $1 - e^{-\Omega(n)}$ until depth $\Omega(2^n)$ [5]. Therefore, the C_ϵ-complexity of outputs of the above monitored circuit with depth t is lower-bounded by $\Omega((\frac{t}{n})^{\frac{1}{5+o(1)}})$ at probability $1 - e^{-\Omega(n)}$ until $t \geq 2^{\Omega(n)}$.

We note that the arguments here do not prove the C_ϵ-complexity growth of a generic output state of the above monitored circuit, because we only looked at special states by choosing unitaries outside the measurement-free paths as identities. It becomes a nontrivial problem even if we perturb the unitaries outside the paths around identities because measurements and the following normalization can significantly enlarge the perturbation. We leave it an open problem to lower-bound the C_ϵ-complexity in monitored circuits in the general setting.

References

[1] Scott Aaronson. *The Complexity of Quantum States and Transformations: From Quantum Money to Black Holes*. 2016. arXiv: 1607.05256 [quant-ph].

[2] Leonard Susskind. "Entanglement is not enough". In: *Fortschritte Phy.* 64.1 (2016), pp. 49–71. DOI: 10.1002/prop.201500095.

[3] Jens Eisert. "Entangling power and quantum circuit complexity". In: *Phys. Rev. Lett.* 127 (2021), p. 020501. DOI: 10.1103/PhysRevLett.127.020501.

[4] Adam R. Brown and Leonard Susskind. "Second law of quantum complexity". In: *Phys. Rev. D* 97.8 (2018), p. 086015. DOI: 10.1103/PhysRevD.97.086015.

[5] Fernando G. S. L. Brandão et al. "Models of quantum complexity growth". In: *PRX Quantum* 2.3 (2021), p. 030316. DOI: 10.1103/PRXQuantum.2.030316.

[6] Jonas Haferkamp et al. "Linear growth of quantum circuit complexity". In: *Nature Phys.* 18.5 (2022), pp. 528–532. DOI: 10.1038/s41567-022-01539-6.

[7] Zhi Li. *Short proofs of linear growth of quantum circuit complexity*. 2022. DOI: https://doi.org/10.48550/arXiv.2205.05668. arXiv: 2205.05668 [quant-ph].

[8] Douglas Stanford and Leonard Susskind. "Complexity and shock wave geometries". In: *Phys. Rev. D* 90 (2014), p. 126007. DOI: 10.1103/PhysRev and 90.126007.

[9] Adam R. Brown et al. "Holographic complexity equals bulk action?" In: *Phys. Rev. Lett.* 116 (2016), p. 191301. DOI: 10.1103/PhysRevLett.116.191301.

[10] Shira Chapman, Hugo Marrochio, and Robert C. Myers. "Complexity of formation in holography". In: *JHEP* 2017.62 (2017), pp. 1–61. DOI: 10.1007/JHEP01(2017)062.

[11] Shira Chapman et al. "Complexity and entanglement for thermofield double states". In: *SciPost Phys.* 6 (2019), p. 034. DOI: 10.21468/SciPostPhys.6.3.034.

[12] Leonard Susskind. "Computational complexity and black hole horizons". In: *Fortschritte Phys.* 64.1 (2016), pp. 24–43. DOI: 10.1002/prop.201500092.

[13] Leonard Susskind. “Three lectures on complexity and black holes”. In: *2018 Prospects in Theoretical Physics summer school*. 2018. DOI: https://doi.org/10.48550/arXiv.1810.11563.

[14] Alexandre Belin et al. “Does complexity equal anything?” In: *Phys. Rev. Lett.* 128 (2022), p. 081602. DOI: 10.1103/PhysRevLett.128.081602.

[15] Yichen Huang and Xie Chen. “Quantum circuit complexity of one-dimensional topological phases”. In: *Phys. Rev. B* 91 (2015), p. 195143. DOI: 10.1103/PhysRevB.91.195143.

[16] Fangli Liu et al. “Circuit complexity across a topological phase transition”. In: *Phys. Rev. Res.* 2 (2020), p. 013323. DOI: 10.1103/PhysRevResearch.2.013323.

[17] Nicole Yunger Halpern et al. “Resource theory of quantum uncomplexity”. In: *Phys. Rev. A* 106 (2022), p. 062417. DOI: 10.1103/PhysRevA.106.062417.

[18] Matthew P. A. Fisher et al. “Random quantum circuits”. In: *Ann. Rev. Cond. Matt. Phys.* 14 (2023), pp. 335–379. DOI: 10.1146/annurev-conmatphys-031720-030658.

[19] Lorenzo Piroli, Christoph Sünderhauf, and Xiao-Liang Qi. “A random unitary circuit model for black hole evaporation”. In: *JHEP* 2020.63 (2020), pp. 1–35. DOI: 10.48550/arXiv.2002.09236.

[20] Patrick Hayden and John Preskill. “Black holes as mirrors: quantum information in random subsystems”. In: *JHEP* 2007.9 (2007), p. 120. DOI: 10.1088/1126-6708/2007/09/120.

[21] Amos Chan, Andrea De Luca, and John T. Chalker. “Solution of a minimal model for many-body quantum chaos”. In: *Phys. Rev. X* 8 (2018), p. 041019. DOI: 10.1103/PhysRevX.8.041019.

[22] Bruno Bertini and Lorenzo Piroli. “Scrambling in random unitary circuits: Exact results”. In: *Phys. Rev. B* 102 (2020), p. 064305. DOI: 10.1103/PhysRevB.102.064305.

[23] Vijay Balasubramanian et al. “Quantum complexity of time evolution with chaotic Hamiltonians”. In: *JHEP* 2020.134 (2020), pp. 1–44. DOI: 10.1007/JHEP01(2020)134.

[24] Fernando G. S. L. Brandão, Aram W. Harrow, and Michał Horodecki. “Local random quantum circuits are approximate polynomial-designs”. In: *Commun. Math. Phys.* 346 (2016), pp. 397–434. DOI: 10.1007/s00220-016-2706-8.

[25] Daniel A. Roberts and Beni Yoshida. “Chaos and complexity by design”. In: *JHEP* 2017.4 (2017), pp. 1–64. DOI: 10.1007/JHEP04(2017)121.

[26] Christoph Dankert et al. “Exact and approximate unitary 2-designs and their application to fidelity estimation”. In: *Phys. Rev. A* 80 (2009), p. 012304. DOI: 10.1103/PhysRevA.80.012304.

[27] David Gross, Koenraad Audenaert, and Jens Eisert. “Evenly distributed unitaries: On the structure of unitary designs”. In: *J. Math. Phys.* 48 (2007), pp. 052104–052104. DOI: 10.1063/1.2716992.

[28] Peter C. Cheeseman, Bob Kanefsky, and William M. Taylor. “Where the really hard problems are”. In: *IJCAI*. 1991, pp. 331–340.

[29] David G. Mitchell, Bart Selman, and Hector J. Levesque. “Hard and easy distributions of SAT problems”. In: *AAAI*. 1992, pp. 459–465.

[30] Michael J. Bremner, Richard Jozsa, and Dan J. Shepherd. “Classical simulation of commuting quantum computations implies collapse of the polynomial hierarchy”. In: *Proc. Roy. Soc. A* 467.2126 (2011), pp. 459–472. DOI: 10.1098/rspa.2010.0301.

[31] Keisuke Fujii and Shuhei Tamate. “Computational quantum-classical boundary of noisy commuting quantum circuits”. In: *Scientific Rep.* 6.1 (2016), pp. 1–15. DOI: 10.1038/srep25598.

[32] Chae-Yeun Park and Michael J. Kastoryano. “Complexity phase transitions in instantaneous quantum polynomial-time circuits”. In: *arXiv:2204.08898* (2022). DOI: https://doi.org/10.48550/arXiv.2204.08898.

[33] Scott Aaronson and Alex Arkhipov. “The computational complexity of linear optics”. In: *Proc. 43rd. Ann. ACM Symp. Th. Comp.* 2011. DOI: 10.1145/1993636.1993682.

[34] Abhinav Deshpande et al. “Dynamical phase transitions in sampling complexity”. In: *Phys. Rev. Lett.* 121.3 (2018), p. 030501. DOI: 10.1103/PhysRevLett.121.030501.

[35] Nishad Maskara et al. “Complexity phase diagram for interacting and long-range bosonic Hamiltonians”. In: *Phys. Rev. Lett.* 129 (2022), p. 150604. DOI: 10.1103/PhysRevLett.129.150604.

[36] Mathias Van Regemortel et al. “Monitoring-induced entanglement entropy and sampling complexity”. In: *Phys. Rev. Res.* 4 (2022), p. L032021. DOI: 10.1103/PhysRevResearch.4.L032021.

[37] Adam Bouland et al. “On the complexity and verification of quantum random circuit sampling”. In: *Nature Phys.* 15.2 (2019), pp. 159–163. DOI: 10.1038/s41567-018-0318-2.

[38] John C. Napp et al. “Efficient classical simulation of random shallow 2D quantum circuits”. In: *Phys. Rev. X* 12 (2022), p. 021021. DOI: 10.1103/PhysRevX.12.021021.

[39] Sarang Gopalakrishnan and Austen Lamacraft. “Unitary circuits of finite depth and infinite width from quantum channels”. In: *Phys. Rev. B* 100 (2019), p. 064309. DOI: 10.1103/PhysRevB.100.064309.

[40] Bruno Bertini, Pavel Kos, and Tomaz Prosen. “Exact correlation functions for dual-unitary lattice models in 1+1 dimensions”. In: *Phys. Rev. Lett.* 123 (2019), p. 210601. DOI: 10.1103/PhysRevLett.123.210601.

[41] Lorenzo Piroli et al. “Exact dynamics in dual-unitary quantum circuits”. In: *Phys. Rev. B* 101 (2020), p. 094304. DOI: 10.1103/PhysRevB.101.094304.

[42] Pieter W. Claeys and Austen Lamacraft. “Ergodic and nonergodic dual-unitary quantum circuits with arbitrary local Hilbert space dimension”. In: *Phys. Rev. Lett.* 126 (2021), p. 100603. DOI: 10.1103/PhysRevLett.126.100603.

[43] Ryotaro Suzuki, Kosuke Mitarai, and Keisuke Fujii. “Computational power of one- and two-dimensional dual-unitary quantum circuits”. In: *Quantum* 6 (2022), p. 631. DOI: 10.22331/q-2022-01-24-631.

[44] Dorit Aharonov. “Quantum to classical phase transition in noisy quantum computers”. In: *Phys. Rev. A* 62 (2000), p. 062311. DOI: 10.1103/PhysRevA.62.062311.

[45] Jens Eisert, Marcus Cramer, and Martin B. Plenio. “Area laws for the entanglement entropy”. In: *Rev. Mod. Phys.* 82 (2010), p. 277. DOI: 10.1103/RevModPhys.82.277.

[46] Brian Skinner, Jonathan Ruhman, and Adam Nahum. “Measurement-induced phase transitions in the dynamics of entanglement”. In: *Phys. Rev. X* 9 (2019), p. 031009. DOI: 10.1103/PhysRevX.9.031009.

[47] Yimu Bao, Soonwon Choi, and Ehud Altman. “Theory of the phase transition in random unitary circuits with measurements”. In: *Phys. Rev. B* 101 (2020), p. 104301. DOI: 10.1103/PhysRevB.101.104301.

[48] David Perez-Garcia et al. “Matrix product state representations”. In: *Quant. Inf. Comp.* 7.5 (2007), pp. 401–430. DOI: https://doi.org/10.26421/QIC7.5-6-1.

[49] Yaodong Li, Xiao Chen, and Matthew PA Fisher. “Quantum Zeno effect and the many-body entanglement transition”. In: *Phys. Rev. B* 98.20 (2018), p. 205136. DOI: 10.1103/PhysRevB.98.205136.

[50] Amos Chan et al. “Unitary-projective entanglement dynamics”. In: *Phys. Rev. B* 99.22 (2019), p. 224307. DOI: 10.1103/PhysRevB.99.224307.

[51] Yaodong Li, Xiao Chen, and Matthew P. A. Fisher. “Measurement-driven entanglement transition in hybrid quantum circuits”. In: *Phys. Rev. B* 100 (2019), p. 134306. DOI: 10.1103/PhysRevB.100.134306.

[52] Michael J. Gullans and David A. Huse. “Dynamical purification phase transition induced by quantum measurements”. In: *Phys. Rev. X* 10 (2020), p. 041020. DOI: 10.1103/PhysRevX.10.041020.

[53] Chao-Ming Jian et al. “Measurement-induced criticality in random quantum circuits”. In: *Phys. Rev. B* 101 (2020), p. 104302. DOI: 10.1103/PhysRevB.101.104302.

[54] Soonwon Choi et al. “Quantum error correction in scrambling dynamics and measurement-induced phase transition”. In: *Phys. Rev. Lett.* 125 (2020), p. 030505. DOI: 10.1103/PhysRevLett.125.030505.

[55] Matteo Ippoliti et al. “Entanglement phase transitions in measurement-only dynamics”. In: *Phys. Rev. X* 11 (2021), p. 011030. DOI: 10.1103/PhysRevX.11.011030.

[56] Ali Lavasani, Yahya Alavirad, and Maissam Barkeshli. “Measurement-induced topological entanglement transitions in symmetric random quantum circuits”. In: *Nature Phys.* 17.3 (2021), pp. 342–347. DOI: 10.1038/s41567-020-01112-z.

[57] Adam Nahum et al. “Measurement and entanglement phase transitions in all-to-all quantum circuits, on quantum trees, and in Landau-Ginsburg theory”. In: *PRX Quantum* 2 (2021), p. 010352. DOI: 10.1103/PRXQuantum.2.010352.

[58] Shengqi Sang and Timothy H. Hsieh. “Measurement-protected quantum phases”. In: *Phys. Rev. Research* 3 (2021), p. 023200. DOI: 10.1103/PhysRevResearch.3.023200.

[59] Pieter W. Claeys et al. “Exact dynamics in dual-unitary quantum circuits with projective measurements”. In: *Phys. Rev. Res.* 4 (2022), p. 043212. DOI: 10.1103/PhysRevResearch.4.043212.

[60] Utkarsh Agrawal et al. “Entanglement and charge-sharpening transitions in U(1) symmetric monitored quantum circuits”. In: *Phys. Rev. X* 12 (2022), p. 041002. DOI: 10.1103/PhysRevX.12.041002.

[61] Xiangyu Cao, Antoine Tilloy, and Andrea De Luca. “Entanglement in a fermion chain under continuous monitoring”. In: *SciPost Phys.* 7 (2019), p. 024. DOI: 10.21468/SciPostPhys.7.2.024.

[62] Qicheng Tang and Wei Zhu. “Measurement-induced phase transition: A case study in the nonintegrable model by density-matrix renormalization group calculations”. In: *Phys. Rev. Res.* 2 (2020), p. 013022. DOI: 10.1103/PhysRevResearch.2.013022.

[63] Yohei Fuji and Yuto Ashida. “Measurement-induced quantum criticality under continuous monitoring”. In: *Phys. Rev. B* 102 (2020), p. 054302. DOI: 10.1103/PhysRevB.102.054302.

[64] Shao-Kai Jian et al. “Measurement-induced phase transition in the monitored Sachdev-Ye-Kitaev model”. In: *Phys. Rev. Lett.* 127 (2021), p. 140601. DOI: 10.1103/PhysRevLett.127.140601.

[65] Takaaki Minato et al. “Fate of measurement-induced phase transition in long-range interactions”. In: *Phys. Rev. Lett.* 128 (2022), p. 010603. DOI: 10.1103/PhysRevLett.128.010603.

[66] Shane P. Kelly et al. “Coherence requirements for quantum communication from hybrid circuit dynamics”. In: *SciPost Phys.* 15 (2023), p. 250. DOI: 10.21468/SciPostPhys.15.6.250.

[67] Pradeep Niroula et al. “Phase transition in magic with random quantum circuits”. In: *Nature Physics* (2024), pp. 1–7. DOI: https://doi.org/10.1038/s41567-024-02637-3.

[68] Geoffrey Grimmett. *Percolation*. Springer, 1999. DOI: 10.1007/978-3-662-03981-6.

[69] Scott Aaronson. “Quantum computing, postselection, and probabilistic polynomial-time”. In: *Proc. Roy. Soc. A* 461.2063 (2005), pp. 3473–3482. DOI: 10.1098/rspa.2005.1546.

[70] Christian Schön et al. “Sequential generation of entangled multiqubit states”. In: *Phys. Rev. Lett.* 95 (2005), p. 110503. DOI: 10.1103/PhysRevLett.95.110503.

[71] Marcus Cramer et al. “Efficient quantum state tomography”. In: *Nature Comm.* 1.1 (2010), p. 149. DOI: 10.1038/ncomms1147.

[72] Adriano Barenco et al. “Elementary gates for quantum computation”. In: *Phys. Rev. A* 52 (1995), pp. 3457–3467. DOI: 10.1103/PhysRevA.52.3457.

[73] Charles H. Bennett et al. “Exact and asymptotic measures of multipartite pure-state entanglement”. In: *Phys. Rev. A* 63 (2000), p. 012307. DOI: 10.1103/PhysRevA.63.012307.

[74] Wolfgang Dür, Guifre Vidal, and J. Ignacio Cirac. “Three qubits can be entangled in two inequivalent ways”. In: *Phys. Rev. A* 62 (2000), p. 062314. DOI: 10.1103/PhysRevA.62.062314.

[75] Lorenzo Piroli, Georgios Styliaris, and J. Ignacio Cirac. “Quantum circuits assisted by local operations and classical communication: transformations and phases of matter”. In: *Phys. Rev. Lett.* 127 (2021), p. 220503. DOI: 10.1103/PhysRevLett.127.220503.

[76] Nathanan Tantivasadakarn et al. “Long-range entanglement from measuring symmetry-protected topological phases”. In: *Phys. Rev. X* 14 (2024), p. 021040. DOI: 10.1103/PhysRevX.14.021040.

[77] Tsung-Cheng Lu et al. “Measurement as a shortcut to long-range entangled quantum matter”. In: *PRX Quantum* 3 (2022), p. 040337. DOI: 10.1103/PRXQuantum.3.040337.

[78] Nathanan Tantivasadakarn, Ashvin Vishwanath, and Ruben Verresen. “Hierarchy of topological order from finite-depth unitaries, measurement, and feedforward”. In: *PRX Quantum* 4 (2023), p. 020339. DOI: 10.1103/PRXQuantum.4.020339.

[79] Vijay Balasubramanian et al. “Quantum chaos and the complexity of spread of states”. In: *Phys. Rev. D* 106 (2022), p. 046007. DOI: 10.1103/PhysRevD.106.046007.

[80] Masahiro Fujii et al. “Characterizing quantum pseudorandomness by machine learning”. In: *arXiv:2205.14667* (2022). DOI: https://doi.org/10.48550/arXiv.2205.14667.

[81] Jonas Haferkamp. *On the moments of random quantum circuits and robust quantum complexity*. 2023. DOI: https://doi.org/10.48550/arXiv.2303.16944.

[82] Frank Verstraete and J. Ignacio Cirac. "Matrix product states represent ground states faithfully". In: *Phys. Rev. B* 73 (2006), p. 094423. DOI: 10.1103/PhysRevB.73.094423.

[83] Mohammad A. Rajabpour. "Post-measurement bipartite entanglement entropy in conformal field theories". In: *Phys. Rev. B* 92 (2015), p. 075108. DOI: 10.1103/PhysRevB.92.075108.

[84] Tokiro Numasawa et al. "EPR pairs, local projections and quantum teleportation in holography". In: *JHEP* 2016.77 (2016). DOI: 10.1007/JHEP08(2016)077.

[85] Stefano Antonini et al. "Holographic measurement and bulk teleportation". In: *JHEP* 2022.12 (2022), pp. 1–76. DOI: 10.1007/JHEP12(2022)124.

[86] Shengqi Sang et al. "Ultrafast entanglement dynamics in monitored quantum circuits". In: *PRX Quantum* 4 (2023), p. 040332. DOI: 10.1103/PRXQuantum.4.040332.

[87] E. Onorati et al. "Mixing properties of stochastic quantum Hamiltonians". In: *Commun. Math. Phys.* 355 (2017), p. 905. DOI: 10.1007/s00220-017-2950-6.

[88] Guifre Vidal and Chris M. Dawson. "Universal quantum circuit for two-qubit transformations with three controlled-NOT gates". In: *Phys. Rev. A* 69 (2004), p. 010301. DOI: 10.1103/PhysRevA.69.010301.

[89] Daniel E. Browne et al. "Phase transition of computational power in the resource states for one-way quantum computation". In: *New J. Phys.* 10.2 (2008), p. 023010. DOI: 10.1088/1367-2630/10/2/023010.

[90] Konrad Kieling and Jens Eisert. "Percolation in quantum computation and communication". In: *Quantum and semi-classical percolation and breakdown in disordered solids*. Lecture Notes in Physics. Springer, 2009. Chap. 10, pp. 287–319. DOI: 10.1007/978-3-540-85428-9.

[91] Konrad Kieling, Terry Rudolph, and Jens Eisert. "Percolation, renormalization, and quantum computing with nondeterministic gates". In: *Phys. Rev. Lett.* 99 (2007), p. 130501. DOI: 10.1103/PhysRevLett.99.130501.

[92] Jonas Haferkamp. "Random quantum circuits are approximate unitary t-designs in depth $O\left(nt^{5+o(1)}\right)$". In: *Quantum* 6 (2022), p. 795. DOI: 10.22331/q-2022-09-08-795.